Tetrahedron 64 (2008) 8449–8463

Contents lists available at ScienceDirect

Tetrahedron

journal homepage: www.elsevier.com/locate/tet

Binding studies of tetrathiafulvalene-calix[4]pyrroles with electron-deficient guests

Kent A. Nielsen [a], Luis Martín-Gomis [b], Ginka H. Sarova [c], Lionel Sanguinet [d], Dustin E. Gross [e], Fernando Fernández-Lázaro [b], Paul C. Stein [a], Eric Levillain [d], Jonathan L. Sessler [e,*], Dirk M. Guldi [c,*], Ángela Sastre-Santos [b,*], Jan O. Jeppesen [a,*]

[a] Department of Physics and Chemistry, University of Southern Denmark, Campusvej 55, DK-5230, Odense M, Denmark
[b] División de Química Orgánica, Instituto de Bioingeniería, Universidad Miguel Hernández, Elche 03202, Alicante, Spain
[c] Institute for Physical and Theoretical Chemistry, Universität Erlangen-Nürnberg, Egerlandstr. 3, 91058 Erlangen, Germany
[d] Université d'Angers, CIMA CNRS, UFR Sciences, 2, bd Lavoisier, 49045 Angers Cedex, France
[e] Department of Chemistry and Biochemistry, The University of Texas at Austin, 1 University Station, A5300, Austin, TX 78712-0165, USA

ARTICLE INFO

Article history:
Received 1 April 2008
Received in revised form 19 May 2008
Accepted 30 May 2008
Available online 5 June 2008

Keywords:
Calix[4]pyrroles
Supramolecular chemistry
Tetrathiafulvalenes
Fullerenes
Molecular switches

ABSTRACT

The neutral *meso*-octamethylporphyrinogen derivative, tetraTTF-calix[4]pyrrole **1** (TTF=tetrathiafulvalene), acts as a multi-faceted receptor in that it interacts with an assortment of different guests in different ways. The conformation of receptor **1** can be reversibly switched between the 1,3-alternate conformation (i.e., **1**, Fig. 1) and the cone conformation (i.e., **1**·Cl^-, Fig. 2) by the repetitive addition of chloride and sodium ions. In this paper, the results of detailed and systematic complexation studies involving both **1** and its chloride-bound complex, **1**·Cl^-, with a variety of guests are described. Receptor **1** binds quasi-planar nitroaromatic guests in its 1,3-alternate conformation, while release of these guests takes place upon addition of chloride anions. On the other hand, spherical fullerene guests are strongly bound by **1**·Cl^-. Finally, it was found that a bidentate guest, consisting of a quasi-planar 2,5,7-trinitro-9-dicyanomethylenefluorene moiety tethered to a spherical C_{60} fullerene, could be recognized by receptor **1** in either its 1,3-alternate or its chloride-bound cone conformation, albeit through very different binding modes.

© 2008 Elsevier Ltd. All rights reserved.

1. Introduction

Calix[4]pyrrole (*meso*-octamethylporphyrinogen) was first made by Baeyer in 1886[1] and reintroduced by Sessler and co-workers[2] as an anion binding agent in 1996. It displays good anion binding affinity and selectivity in apolar solvents and can be prepared via a simple, one-step reaction. This has made it an attractive platform for further modification. For instance, ongoing efforts to improve the anion binding affinity and selectivity of calix[4]pyrroles have resulted in various structural modifications to the basic tetrapyrrolic skeleton,[3,4] including functionalized derivatives that act as rudimentary colorimetric chemosensors for various negatively charged analytes.[5] Although some efforts have been carried out to combine calix[4]pyrroles with redox-active units, such as ferrocene,[6] in order to generate electrochemically active sensors, they were not fully successful until 2003[7] when a chemosensor based on a redox-active tetrathiafulvalene[8,9] (TTF) unit in combination with a pseudocalix[4]pyrrole[10] system was reported. In the context of this work, it was found that attaching one redox-active TTF unit directly to the pseudocalix[4]pyrrole core produced a receptor with enhanced binding affinities toward Br^-, Cl^-, and F^- ions. However, the inherent instability of the underlying pseudocalix[4]pyrrole system precluded further studies of this first generation system. Accordingly, *meso*-octamethylcalix[4]pyrrole derivatives bearing TTF units annulated to the β pyrrolic positions of the *meso*-octamethylcalix[4]pyrrole core were prepared.[11] Since TTF and its derivatives are good electron donors capable of forming donor/acceptor complexes,[8] it was expected that the resulting modified calix[4]pyrroles, such as the tetraTTF-calix[4]pyrrole host **1** (Fig. 1), would be capable of interacting with electron-deficient guests. As detailed in two recent communications,[12] not only was this expectation met, it was also found that the complexation and decomplexation processes (Fig. 2) could be controlled through the absence/presence of Cl^- ions.

In this follow-up paper, we elaborate on this fundamental finding and detail the manner in which the tetraTTF-calix[4]pyrrole

* Corresponding authors. Tel.: +1 512 471 5009; fax: +1 512 471 7550 (J.L.S.).
E-mail addresses: sessler@mail.utexas.edu (J.L. Sessler), guldi@chemie.uni-erlangen.de (D.M. Guldi), asastre@umh.es (Á. Sastre-Santos), joj@ifk.sdu.dk (J.O. Jeppesen).

0040-4020/$ – see front matter © 2008 Elsevier Ltd. All rights reserved.
doi:10.1016/j.tet.2008.05.141

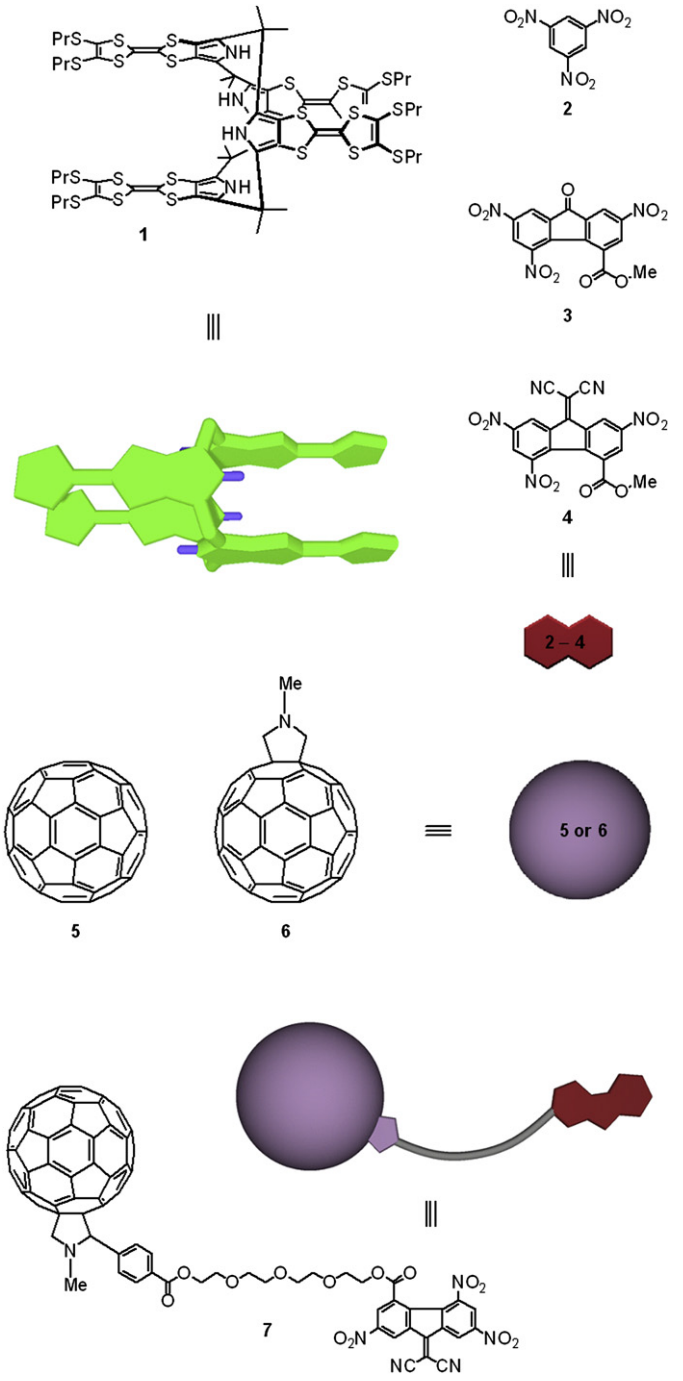

Figure 1. Line drawing of the receptor tetraTTF-calix[4]pyrrole **1**, shown as a three-dimensional representation; a cartoon representation of **1** in its 1,3-alternate conformation, and line drawings of trinitrobenzene **2**, MTNFC **3**, MTNDMFC **4**, C_{60} **5**, NMF **6**, and TNDCF–C_{60} **7** and their corresponding cartoon representations.

1 acts as a controllable 'molecular switch'. Specifically, we describe detailed and systematic complexation studies carried out between both the neutral tetraTTF-calix[4]pyrrole[11,13] receptor **1** (Fig. 1) and its chloride-bound cone complex,[13] **1**·Cl^- (Fig. 2), with a variety of different guests, namely (i) tetraalkylammonium cations (TBA^+ and TEA^+, studied as their chloride salts), (ii) quasi-planar nitroaromatic guest trinitrobenzene (TNB, **2**), methyl 2,5,7-trinitrofluorenone-4-carboxylate[14] (MTNFC, **3**), and methyl 2,5,7-trinitrodicyanomethylenefluorene-4-carboxylate[14] (MTNDMFC, **4**), (iii) spherical guest fullerene (C_{60}, **5**) and its derivative *N*-methylfulleropyrrolidine[15] (NMF, **6**), and finally (iv) the bidentate guest

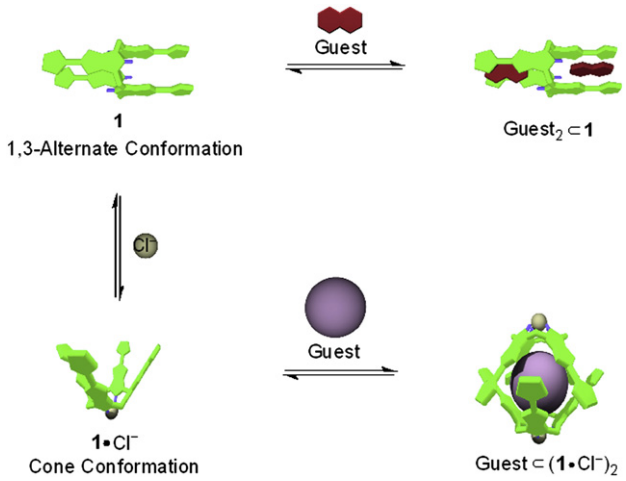

Figure 2. Complexation between the receptor **1** and quasi-planar electron-deficient aromatic guests is favored in the 1,3-alternate conformation, whereas the receptor in the presence of chloride anions—cone conformation (**1**·Cl^-)—preferentially binds electron-deficient spherical guests.

2,5,7-trinitro-9-dicyanomethylenefluorene–C_{60}[14] (TNDCF–C_{60}, **7**). As inferred from ^{1}H NMR, absorption, and emission spectroscopic studies, as well as electrochemical measurements, the tetraTTF-calix[4]pyrrole receptor **1** acts as an effective receptor for neutral electron-deficient guests and chloride anions in solution. However, depending on the guests in question, these two binding processes can act in concert or in opposition. This makes receptor **1** a prototype of a chemically controllable molecular recognition agent.

2. Results and discussion

We have previously shown[13] that the tetraTTF-calix[4]pyrrole receptor **1** exists (Fig. 2) predominantly in the 1,3-alternate conformation. However, in halogenated solvents, **1** binds chloride anions very strongly—a binding constant of $2.5\times10^6\ M^{-1}$ has been reported[11,13] for the complexation of **1** with chloride in 1,2-dichloroethane (DCE) at 298 K—leading it to adopt a cone conformation **1**·Cl^-. This conformational change can be easily followed using ^{1}H NMR spectroscopy, since the resonances associated with the NH protons in **1**·Cl^- are shifted to lower field by 3.67 ppm ($CDCl_3$, 298 K) when compared to the NH signals in the free receptor **1**. In addition, the signal corresponding to the methyl groups at the *meso*-position of the calix[4]pyrrole ring system, observed as one singlet at δ=1.62 ppm in the free receptor **1**, becomes separated into two broad singlets that are shifted downfield by $\Delta\delta$=0.37 and 0.17 ppm, respectively, upon the addition of tetrabutylammonium chloride (TBACl). Such findings are consistent with four of the eight *meso*-methyl groups pointing in the direction of the sulfur atoms in the TTF units with the other four *meso*-methyl groups pointing in the direction of the chloride-anion binding site (i.e., the pyrrolic NH rim).

In the absence of anionic species, **1** preferentially binds quasi-planar electron-deficient aromatic guests[11] that are capable of forming stabilizing charge-transfer (CT) and hydrogen bonding interactions. This leads to the formation of sandwich-like complexes having a receptor/guest stoichiometry of 1:2 (Fig. 2). However, in the presence of chloride (i.e., **1**·Cl^-), this receptor binds preferentially electron-deficient spherical guests,[12a] such as fullerene, by encapsulating the guest in a 2:1 ratio (Fig. 2). These anion-triggered differences in selectivity are reflected in easy-to-visualize color differences.

For reasons of solubility, the solution state studies of the tetraTTF-calix[4]pyrrole receptor **1** were carried out in dichloromethane[16] or a mixture of dichloromethane and toluene.[17] These

solvents, along with chloroform, were used for most of the studies described in this paper.

2.1. Conformational control: addition of chloride anion and binding of the tetrabutylammonium cation

The ^{1}H NMR spectrum ($CDCl_3$, 200 MHz, 298 K) of receptor **1** shows (Fig. 3B) one broad singlet at δ=7.15 ppm integrating to 4H, which can be assigned to the four chemically equivalent NH protons' resonance. Addition of 0.5 equiv of TBACl to a solution of receptor **1** leads to an equilibrium favoring the cone-like conformation via formation of the chloride-anion complex, **1**·Cl$^-$ (Fig. 3A). The conformational change of the receptor can easily be observed in the ^{1}H NMR spectrum, where two different signals are observed for the NH protons, one at δ=7.15 ppm, corresponding to the uncomplexed receptor (**1**), and the other at δ=10.82 ppm, corresponding to the chloride complex (**1**·Cl$^-$). This finding is taken as evidence that the exchange between the complexed and uncomplexed species is slow on the ^{1}H NMR timescale. After the addition of 1.0 equiv of TBACl, only the signal at δ=10.82 ppm, corresponding to complexed receptor (**1**·Cl$^-$), is observed in the ^{1}H NMR spectrum under these conditions, as would be expected for a complex where the chloride anion is bound very tightly.[13]

Additionally, the resonance ascribable to the SCH_2 protons appears as a triplet at δ=2.82 ppm integrating to 16H in the absence of chloride anion, while the remaining resonances from the propyl chains, integrating to 16H and 24H, respectively, are observed at 1.68 (CH_2) and 1.04 ppm (CH_3) (Fig. 3C). The signal from the *meso*-methyl groups resonates as a broad singlet at δ=1.62 ppm (Fig. 3C). After the addition of TBACl, the SCH_2 signal becomes somewhat broadened but continues to resonate at δ=2.82 ppm. The resonances corresponding to the *meso*-methyl groups are shifted to lower field, and are split into two broad signals appearing at δ=1.99 and 1.79 ppm, respectively. An ^{1}H–{^{1}H}NOE NMR experiment was carried out to assign the resonances associated with the two non-equivalent methyl groups. Irradiation of the NH protons (δ=10.82 ppm) led to a significant enhancement in the signal at δ=1.99 ppm and only a smaller enhancement in the signal at δ=1.79 ppm. These results are consistent with the resonance at δ=1.99 ppm corresponding to the methyl group that is oriented in the direction of the anion binding site (i.e., the pyrrolic NH rim), whereas that at δ=1.79 ppm corresponds to the methyl group pointing in the direction of the sulfur atoms of the pyrrolo-TTF units. Interestingly, the ^{1}H NMR spectrum of a 1:1 mixture of the receptor **1** and TBACl revealed a 0.37 ppm upfield shift in the signals associated with the NCH_2 protons of the tetrabutylammonium cation (TBA^+), which normally resonate at δ=3.38 ppm in pure TBACl. This observation can most likely be attributed to binding of the tetrabutylammonium cations inside the cavity of the receptor **1**·Cl$^-$, an effect that has been seen in the case of simple calix[4]pyrrole, both in solution and in solid state.[18]

2.1.1. Electrochemical investigation

Compound **1** was also characterized using cyclic and thin layer cyclic voltammetry (TLCV). Figure 4 (recorded at 0 equiv added guest) shows the deconvoluted voltammogram of **1** and reveals two oxidation processes at −0.04 and 0.53 V (vs Fc^+/Fc), respectively. In the positive direction, a separation of the first oxidation process is observed with an intensity ratio of 1:3. This ratio is maintained over the entire concentration range used in this study.

This behavior, already observed in the literature for a similar system,[19] was interpreted in terms of an interaction between the TTF donor moieties either as a result of conjugation or taking place through space.[20] In the present system, it could simply reflect the fact that the four TTF units are fused to the calixpyrrole core. Such structural proximity is expected to result in a higher degree of overlap and possible stabilization of the monoradical cation. After oxidation of the first TTF unit, the degree of interaction decreases, which leads to a stabilization of the HOMO level. Therefore, the peak associated with further oxidation (i.e., of the remaining three TTF units) is now shifted to a more positive potential compared to the oxidation potential of the first TTF unit.

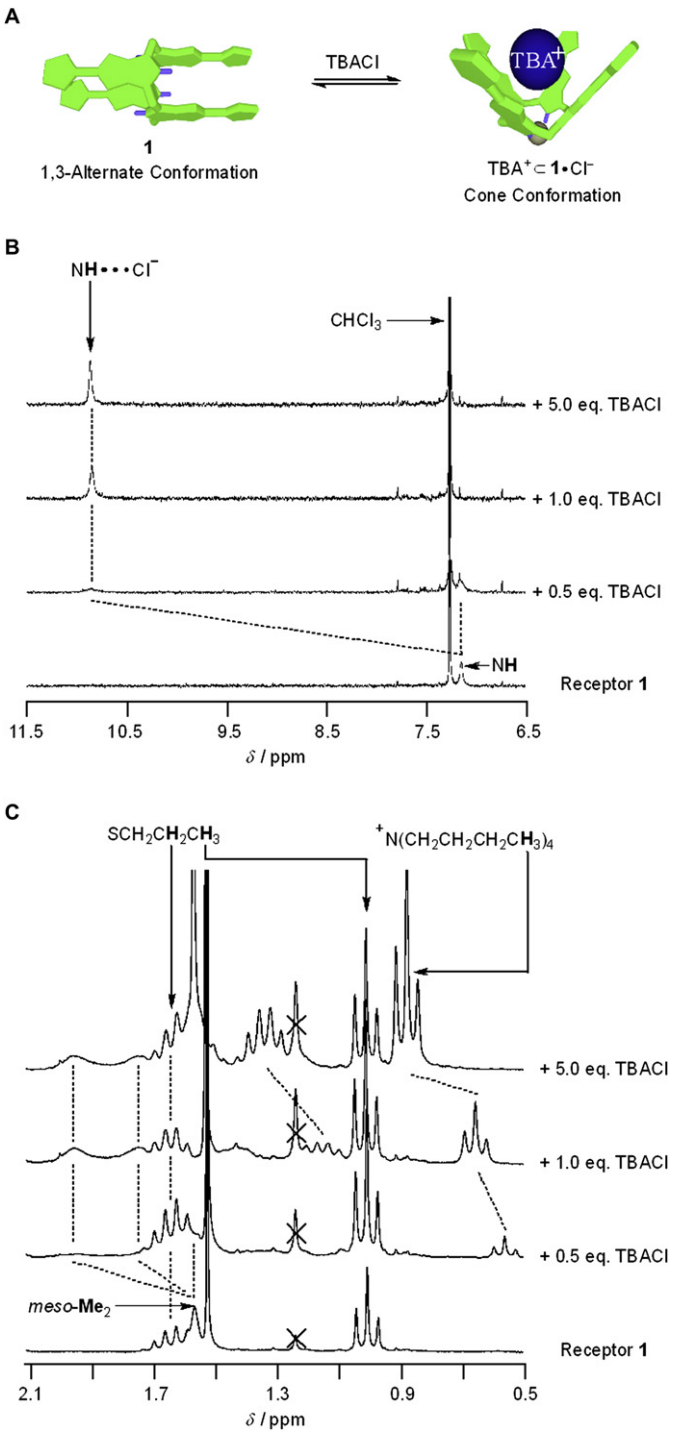

Figure 3. (A) Mechanistic scheme illustrating the proposed conformational switching of receptor **1** between its anion-free 1,3-alternate conformation (**1**) and the corresponding anion-bound cone conformation (**1**·Cl$^-$) that takes place upon the addition of TBACl. (B) Partial ^{1}H NMR ($CDCl_3$, 200 MHz) spectra showing the shift of the NH proton upon the addition of TBACl. (C) Partial ^{1}H NMR ($CDCl_3$, 200 MHz) spectra showing the shift and splitting of the *meso*-Me_2 protons upon the addition of TBACl to a solution of receptor **1**.

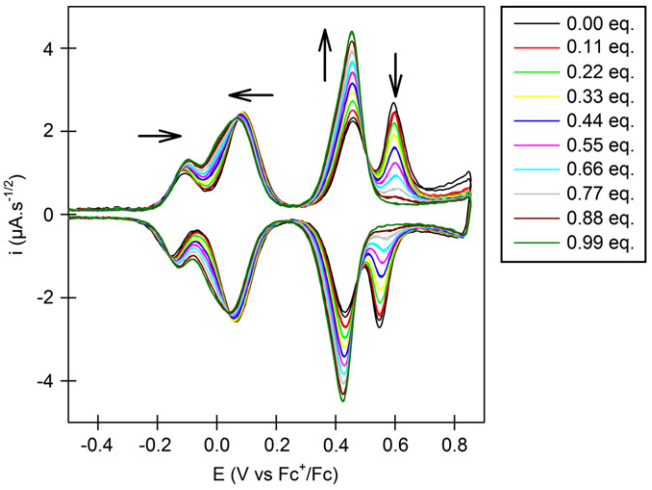

Figure 4. Deconvoluted cyclic voltammograms of receptor **1** (75 μM in CH_2Cl_2/toluene (8:2 v/v)) at 200 mV s^{-1} obtained after the addition of successive aliquots of TBACl (Reference electrode: Fc^+/Fc; supporting electrolyte: TBAHFP (0.1 M)).

The second oxidation process is manifested in terms of different electrochemical behaviors. In this case, as observed for the first process, a separated wave is observed. However, this second oxidation wave is sharper and is thought to reflect the absorption phenomena. This hypothesis was confirmed by TLCV measurements carried out at a low scan rate.[21] Unfortunately, in spite of all attempts, this absorption feature is always present and is seen as soon as the first TTF dication is formed.

The addition of chloride anions to **1** in solution induces large changes in the electrochemistry (cf. Fig. 4). For the first oxidation process, a decrease in the separation was observed, namely from ΔE=200 mV without chloride to ΔE=160 mV with chloride. This behavior is consistent with a reduction in the interaction between the TTF units and is what would be expected for a system that has undergone a chloride-anion induced change in conformation.

In the case of the second oxidation process, the addition of chloride leads to the disappearance of the second peak and a corresponding enhancement in the size of the first peak. This electrochemical behavior is characteristic of a molecular system where all the TTF radical cations are oxidized to the corresponding TTF dication at the same potential. It is thus fully consistent with the formation of a chloride-anion complex **1**·Cl^-. In other words, when considered in concert, the electrochemical studies support the spectroscopic analyses and provide further evidence that the addition of chloride to the tetraTTF-calix[4]pyrrole **1** induces a conformation change from 1,3-alternate to the cone conformation.

2.2. Determination of the binding constants between the receptor 1 and Cl^- and between the tetrabutylammonium cation and 1·Cl^-

To quantify the interaction of **1** with chloride, we utilized isothermal titration calorimetry (ITC).[22,23] When titrating tetraethylammonium chloride (TEACl) or TBACl (~30 mM) into a dichloromethane solution of the receptor **1** (1 mM), we observed heat signatures that could be fitted to a clean 1:1 binding profile. The resulting thermodynamic data (Table 1) are similar for both TEACl and TBACl with enthalpy values of −11.7 and −11.0 kcal mol^{-1} and binding constants (K_a) of 8.7×10^5 and 3.6×10^5 M^{-1} being calculated between **1** and these two salts, respectively, in dichloromethane. This behavior is divergent from that of *meso*-octamethylcalix[4]pyrrole,[1] where we observed a 2 order of magnitude difference in the K_a values between TEACl and TBACl under identical conditions.[18b] Possible explanations for this anomaly are that (i) a higher affinity for anions could be masking the effect of the weaker cation/calix[4]pyrrole interaction or (ii) the electron-rich cavity formed from **1** as a result of anion complexation is large enough to encapsulate equally either TEA^+ or TBA^+ cations. While further study will be required to address this issue, we currently favor the latter explanation.

Table 1
Binding constants[a] (K_a, M^{-1}) and thermodynamic parameters (kcal mol^{-1}) corresponding to the interactions between the receptor **1** and chloride anions in the form of either TEA^+ or TBA^+ salts as determined by ITC[b] at 298 K in CH_2Cl_2

Salt	[**1**] (mM)	$T\Delta S$	ΔH	ΔG	K_a
TEACl	1.0	−3.55	−11.66	−8.11	8.7×10^5
TBACl	1.0	−3.43	−11.01	−7.58	3.6×10^5
TBACl	0.1	−1.78	−9.95	−8.17	9.8×10^5

[a] Estimated errors are <10%.
[b] The receptor was titrated with the salts in question so as to obtain the heat effects corresponding to complexation. The net heat effect was determined by subtracting the heat traces for the appropriate background titration.

As evident from the shift of the TBA^+ methyl protons in Figure 3C, there seems to be an interaction between the TBA^+ cation and **1** in solution. Therefore, a titration experiment was carried out in order to determine the binding constant between the TBA^+ cation and **1**·Cl^-. The conformation of the receptor was converted from its initial 1,3-alternate conformation **1** into the corresponding cone conformation **1**·Cl^- via the addition of excess potassium chloride and 6.0 equiv of dicyclohexano-18-crown-6 (**8**) (Fig. 5).[24] The ^1H NMR spectrum of this mixture was consistent with this conformational switching process being complete (i.e., near-quantitative conversion to **1**·Cl^-). Accordingly, this solution was titrated into a solution of tetrabutylammonium hexafluorophosphate (TBAHFP).[25] By following the changes (Fig. 5B) in the chemical shift for the resonances associated with the methyl protons of the TBA^+ cation upon addition of an increasing amount of the receptor **1**·Cl^- at 298 K, the binding constant for this 1:1 interaction could be determined using nonlinear curve fitting (Fig. 5C); this yielded a K_a value of 7.4×10^3 M^{-1} for the interaction between the TBA^+ cation and **1**·Cl^-. A continuous variation ^1H NMR spectroscopic experiment was also carried out to determine the stoichiometry of the binding between the TBA^+ cation and the receptor **1**·Cl^-. The Job plot obtained in this way (Fig. 5C, inset) exhibited a maximum at a mole ratio of 0.46, consistent with a 1:1 interaction.

2.3. Reversible switching between the neutral receptor 1 and $TBA^+\subset$1·Cl^-

To examine further the extent to which the presence or absence of chloride anion in solution could mediate the conformation of receptor **1**, an ^1H NMR experiment was carried out that involved the repeated addition of first chloride anion (as its TBA^+ salt) followed by sodium cation (as its sodium tetraphenylborate, NaTPB, salt) to a solution of receptor **1**. This sequence of events (Fig. 6A) serves to switch the receptor **1** between its 1,3-alternate conformation (**1**) and the chloride-bound cone conformation (**1**·Cl^-). As above, receptor **1** was converted to the cone conformation by the addition of TBACl. Addition of 2 equiv of Na^+ (as its TPB^- salt) then caused sodium chloride to precipitate from the NMR solution. An ^1H NMR spectrum (Fig. 6B and C) recorded subsequently revealed that the NH protons, as well as the methyl protons in the *meso*-position, reverted back to essentially their initial positions (δ=7.15 and 1.61 ppm for these two sets of signals, respectively). This is as expected for a precipitation event that serves to remove chloride (NaCl) and returns receptor **1** back to its initial 1,3-alternate conformation. Repeated addition of TBACl

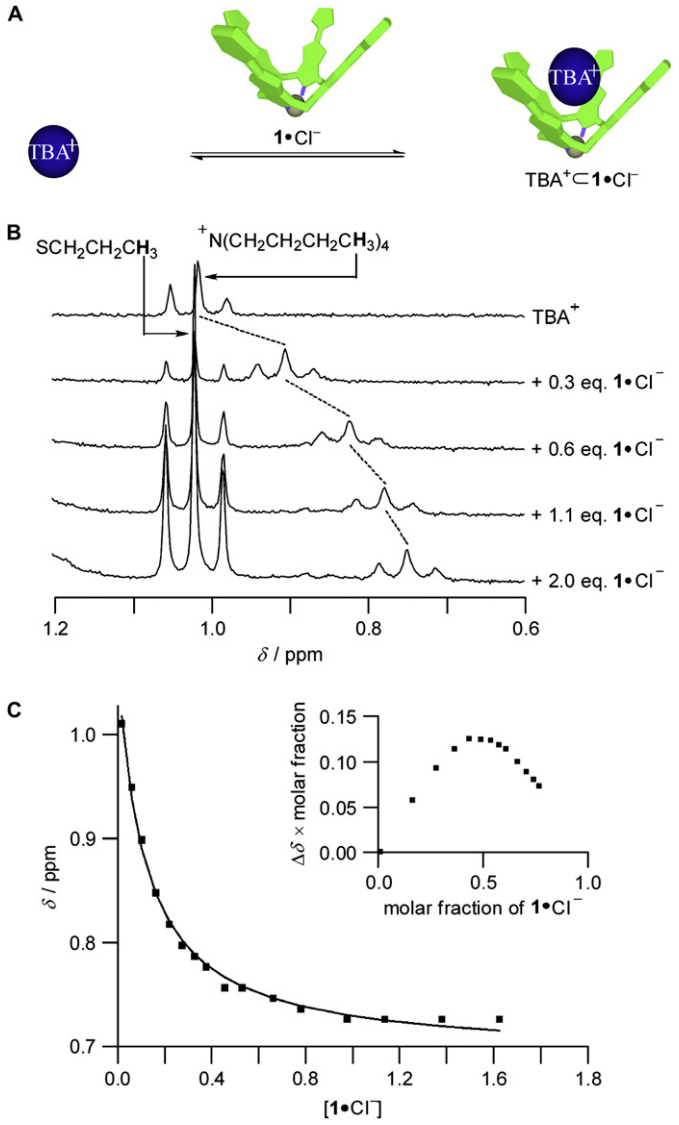

Figure 5. (A) Mechanistic scheme illustrating the proposed binding of the TBA^+ cation by the receptor $\mathbf{1}\cdot Cl^-$. (B) Partial ^1H NMR ($CDCl_3$, 200 MHz) spectra showing the upfield shift of the methyl protons from the TBA^+ cation, upon titration with an increasing amount of receptor **1** in its anion-bound cone conformation, $\mathbf{1}\cdot Cl^-$. (C) ^1H NMR titration curve showing the changes in the signals of the methyl protons of the TBA^+ cation seen upon the addition of increasing the amounts of $\mathbf{1}\cdot Cl^-$ to a solution of tetrabutylammonium hexafluorophosphate. The inset shows a Job plot that is consistent with a 1:1 binding stoichiometry for the interaction of $\mathbf{1}\cdot Cl^-$ with the TBA^+ cation.

followed by the subsequent addition of NaTPB resulted in the continuation of the controlled conformational switching of the receptor **1** between its 1,3-alternate and cone conformations (**1** vs $\mathbf{1}\cdot Cl^-$), as can be inferred from Figure 6.

2.4. Complexation between the receptor 1 and the quasi-planar aromatic guests 2–4

The interactions between the receptor **1** and guests **2**–**4** were investigated in solution using absorption, emission, and ^1H NMR spectroscopies, as well as cyclic voltammetry. The findings from these studies are detailed below.

2.4.1. Absorption spectroscopic investigations

Separately, receptor **1** and guests **2**–**4** do not display any notable absorption bands in the visible spectral region greater than λ=550 nm (Fig. 7). However, the addition of 2 equiv of any one of

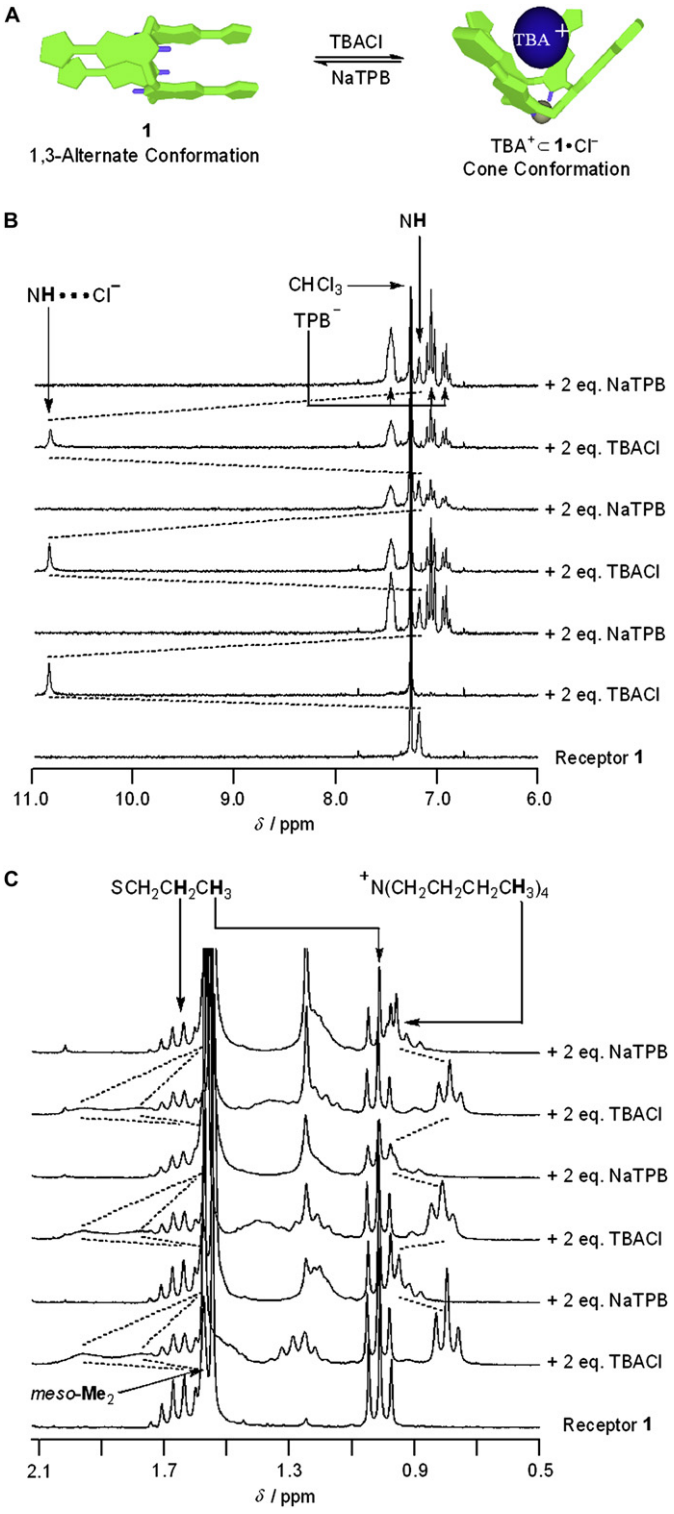

Figure 6. (A) Mechanistic scheme illustrating the proposed reversible switching between receptor **1** and $TBA^+\subset\mathbf{1}\cdot Cl^-$. (B) and (C) Partial ^1H NMR spectra ($CDCl_3$, 200 MHz) illustrating the reversible switching of the NH proton, the *meso*-Me_2 signals of the receptor **1**, and the methyl protons from the TBA^+ cation, seen upon repeated addition of chloride anions and sodium cations to a solution of receptor **1**.

the guests **2**–**4** to a dichloromethane solution of **1** results in an immediate color change and the concomitant appearance of new absorption bands in the visible-near-infrared region of the electronic spectrum. In the case of TNB (**2**), a color change from yellow to green and the appearance of one new absorption band at

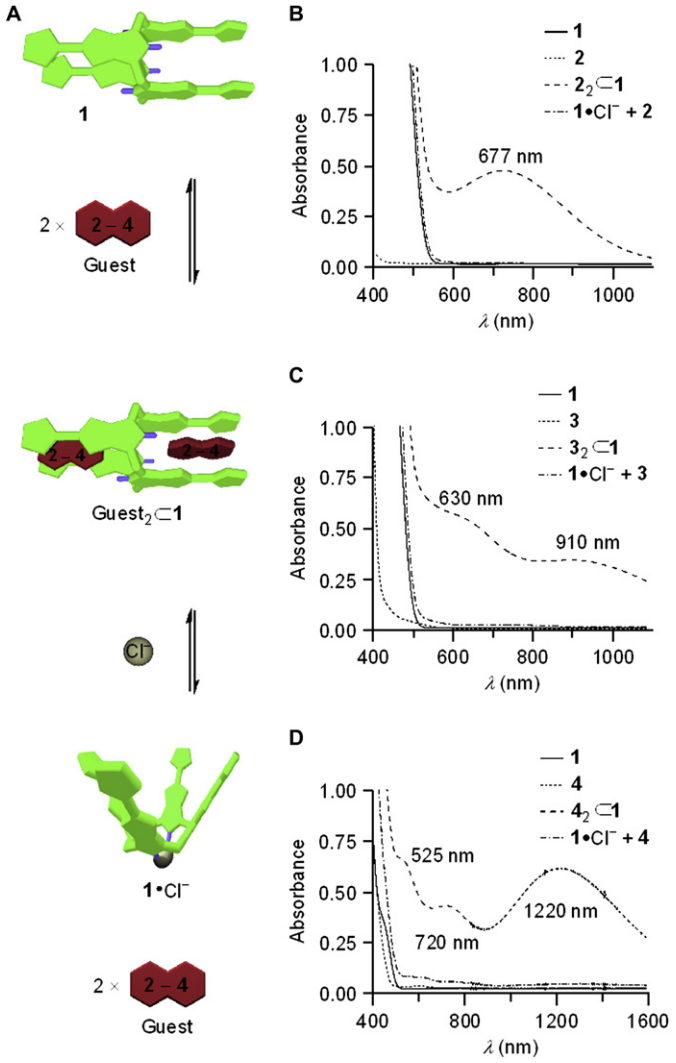

Figure 7. (A) Mechanistic scheme illustrating the proposed complexation events involving receptor **1** and guests **2**–**4** observed in the absence and presence of chloride anions, respectively. (B)–(D) Absorption spectra recorded in CH_2Cl_2 of **1** (1.0 mM in the case of **2** and **3**, and 0.25 mM in the case of **4**), 2 equiv of the guests **2**–**4**, and mixtures of receptor **1** and 2 equiv of the guests **2**–**4** in the absence and presence of chloride anions.

λ_{max}=677 nm (ε=477 M^{-} cm^{-1}) were observed (Fig. 7B); in the case of MTNFC **3**, two weak absorption bands, at λ_{max}=630 and 910 nm (ε=553 and 335 M^{-1} cm^{-1}), respectively, were observed (Fig. 7C); and for MTNDMFC **4**, a color change from yellow to brown was seen, along with the appearance of three absorption bands at λ_{max}=525, 720, and 1220 nm (ε=2630, 1670, and 2420 M^{-1} cm^{-1}), respectively (Fig. 7D). These changes in the absorption spectra are believed to arise from CT interactions between the TTF donor units in receptor **1** and the electron-deficient species **2**–**4**, which act as acceptors. Presumably, this CT interaction is enhanced by the guest/calix[4]pyrrole hydrogen bonding interaction involving the two NH protons from the receptor **1** and one or more of the hydrogen bonding acceptor groups in the guests **2**–**4**.[26]

Addition of 2 equiv of TBACl to solutions of **1** containing 2 equiv of any of the guests **2**–**4** causes the color of the solution to revert back to the original yellow. This transformation is accompanied by the disappearance (Fig. 7B–D) of all absorption bands above 550 nm. This change in naked eye-detectable color and visible spectral features is rationalized in terms of the chloride anions present in solution being in competition with the electron-deficient guests for the NH protons of **1** and therefore inducing an equilibrium between the 1,3-alternate and the cone conformations. Moreover, because the hydrogen bonding interactions with Cl^{-} are stronger than the interactions associated with the neutral, electron-deficient guests **2**–**4** (as reflected in the high binding constant between **1** and chloride anion, vide supra), the equilibrium is largely shifted in favor of the cone conformation.

2.4.2. ^{1}H NMR spectroscopic studies

Analyses of the interactions between receptor **1** in its 1,3-alternate conformation and guests **2**–**4** were also carried out using ^{1}H NMR spectroscopy. The ^{1}H NMR spectrum (300 MHz, $CDCl_3$, 298 K) of **1** reveals (Fig. 8A) a signal at δ=7.15 ppm that is ascribed to the NH protons. On the other hand, the ^{1}H NMR spectrum (Fig. 8B) of guest **2** is characterized by one singlet at δ=9.37 ppm that is readily assigned to the aromatic protons (Ar–H). Upon the addition of 2 equiv of guest **2** to a solution of **1** (Fig. 8C), the signals corresponding to the NH protons are shifted to δ=7.79 ppm ($\Delta\delta$=0.69 ppm), a process fully consistent with the presence of hydrogen bonding interactions involving the host and the guest(s). Under these conditions, the Ar–H protons of **2** are found to resonate at δ=9.20 ppm ($\Delta\delta$=−0.17 ppm), presumably as a consequence of being sandwiched between two shielding TTF subunits.

Upon the addition (Fig. 8D) of 2 equiv of TBACl, the signal for the Ar–H protons in **2** reverts almost completely back to its initial position (δ=9.35 ppm), as would be expected if the guest is released. Consistent with this chloride-anion 'switched' conformational change and release of the bound guest **2**, the NH protons

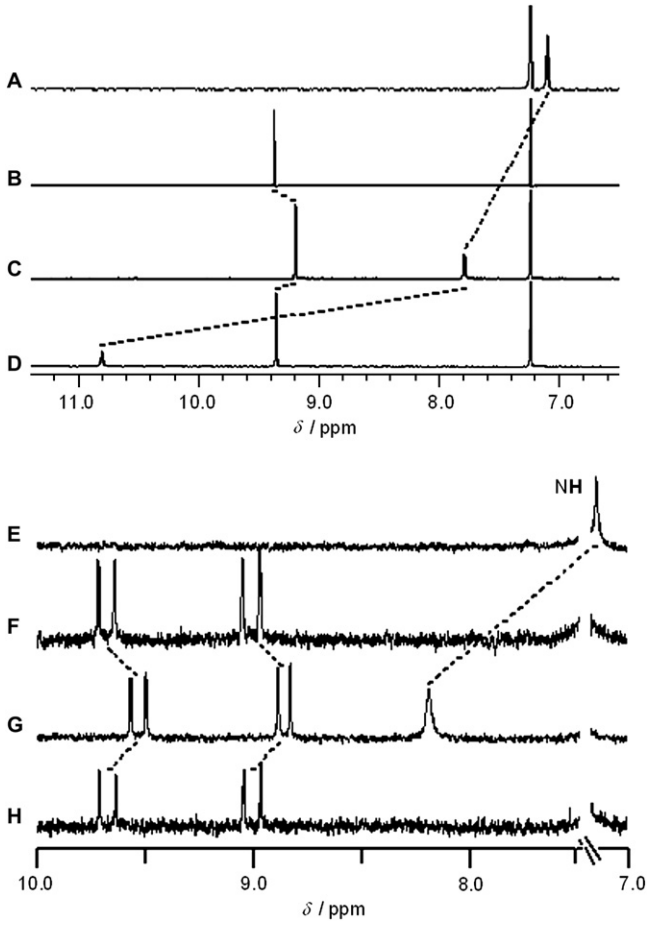

Figure 8. Partial ^{1}H NMR spectra ($CDCl_3$, 300 MHz) of: (A) receptor **1**, (B) TNB **2**, (C) receptor **1**+2 equiv of TNB **2**, (D) receptor **1**+2 equiv of TNB **2**+2 equiv of TBACl, (E) receptor **1**, (F) MTNDMFC **4**, (G) receptor **1**+2 equiv of MTNDMFC **4**, (H) receptor **1**+2 equiv of MTNDMFC **4**+2 equiv of TBACl.

Table 2
Binding constants[a] (K_1 and K_2, M^{-1}) corresponding to the interactions between receptor **1** and guests **2**–**4** as determined from visible absorption or ^{1}H NMR spectroscopic titrations carried out at room temperature

Guest	K_1	K_2
2	20[b]	900[b]
3	160[b]	516[b]
4	1200[c]	5160[c]

[a] Estimated errors are <15%.
[b] Determined using ^{1}H NMR spectroscopy in $CDCl_3$ at 298 K.
[c] Determined using absorption spectroscopy in CH_2Cl_2 at 295 K.

of **1** are seen to shift to even lower field (δ=10.80 ppm), as would be expected given the strong hydrogen bonding interactions between the calix[4]pyrrole NH's and chloride anion present in **1**·Cl^-. Similar behavior was seen with guest **4**, as illustrated in Figure 8E–H.

Job plots obtained[27] from continuous variation ^{1}H NMR spectroscopic experiments, involving receptor **1** in its 1,3-alternate conformation and guests **2**–**4**, were found to exhibit maxima in the 0.59–0.60[28] molar ratio region, a finding that is consistent with a 1:2 binding stoichiometry between the receptor and the guest.

In order to determine the binding constants (K_1 and K_2) for the 1:2 complexes (guest$_2$⊂**1**), standard titration[27] experiments were carried out by following either the change in absorbance of the CT bands formed upon complexation or by observing the change in the resonance associated with the NH protons in the corresponding ^{1}H NMR spectra. The data were analyzed using standard curve fitting methods (i.e., Connors 1:2 model[29]); this gave the values listed in Table 2.

Although the data in Table 2 do reflect slightly different measurement conditions (T=298 vs 295 K, $CDCl_3$ vs CH_2Cl_2), to the extent that the effects in question are small, it is clear that guest **4** has the strongest affinity toward the receptor **1**, whereas guest **2** has the weakest affinity toward receptor **1**. Given the relative size of the species involved, this difference is rationalized in terms of electronic and orbital overlap considerations, rather than the more-classical steric terms. In other words, it is the ability to stabilize (i) hydrogen bonding and (ii) strong donor/acceptor interactions with **1**, as opposed to simply fitting in its binding pockets, that appears to be determinative.

2.4.3. Photophysical investigations

To complement the above binding studies, we followed the fluorescence of **4** as a function of its interaction with **1**. Implicit in these analyses are electron transfer reactions that might involve the electron-accepting guest **4** and the electron-donating host **1**. Such electron transfer events are expected to lead to quenching of the fluorescence. Indeed, when, for example, dichloromethane solutions of **4** were titrated with increasing quantities of **1**, a gradual decrease in the fluorescence intensity of **4** was observed (Fig. 9). Plotting the intensities at the 540 nm fluorescence maximum versus the concentration of **1** and fitting them to a 1:2 binding equation afforded K_1 and K_2 values of 1.0×10^4 and 2.1×10^4 M^{-1} for the formation of **4**⊂**1** and (**4**)$_2$⊂**1**, respectively. In the presence of chloride anion, no discernible interactions were found between **4** and **1**·Cl^-.

Femtosecond resolved transient absorption measurements were also carried out, which provided support for the proposed electron transfer-based fluorescence quenching processes. Two absorption bands at 535 and 870 nm are formed concomitantly upon laser pulse excitation of (**4**)$_2$⊂**1** at 387, 730, or 1200 nm. These features resemble the absorption spectrum of the one-electron reduced radical anion of MTNDMFC **4**, which was generated independently in pulse radiolytic reduction experiments with **4**. The corresponding one-electron oxidized radical cation of TTF was found to absorb in the 400 nm spectral region. Applying a first order kinetic model to the transient decays in the 400, 535, and 870 nm regions allowed a radical ion pair lifetime of ca. 2 ps to be estimated.

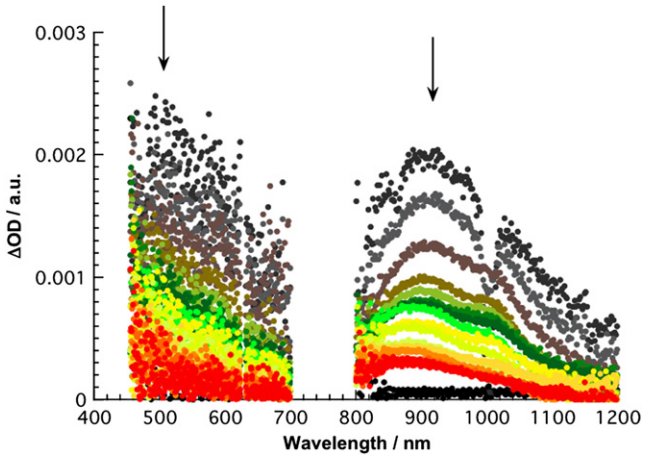

Figure 9. Differential absorption spectra (visible and near-infrared) obtained upon femtosecond flash photolysis (730 nm) of (**4**)$_2$⊂**1** in nitrogen saturated CH_2Cl_2 with several time delays between 0 and 10 ps at room temperature—arrows indicate the evolution of the differential changes.

2.4.4. Electrochemical investigations

The complexation between receptor **1** and MTNDMFC (**4**) can also be followed by electrochemistry as illustrated in Figure 10. For instance, the addition of **4** induces a slight positive shift in the shoulders of the first oxidation wave for **1** (around 34 mV). This effect is associated with a small increase in the intensity of the second oxidation peak. In view of the spectroscopic results detailed above, these observations are rationalized in terms of guest **4** being complexed by host **1**. In this case, the positive shift would be due to the presence of donor/acceptor interactions induced or enhanced by complexation. Surprisingly, this positive shift is not observed in the case of the second peak associated with the first oxidation process. Such a finding is rationalized in terms of an increase in absorption to the electrode taking place during the successive addition of **4**. In the negative direction, the intensities of the redox waves associated with reduction of **4** were seen to increase upon

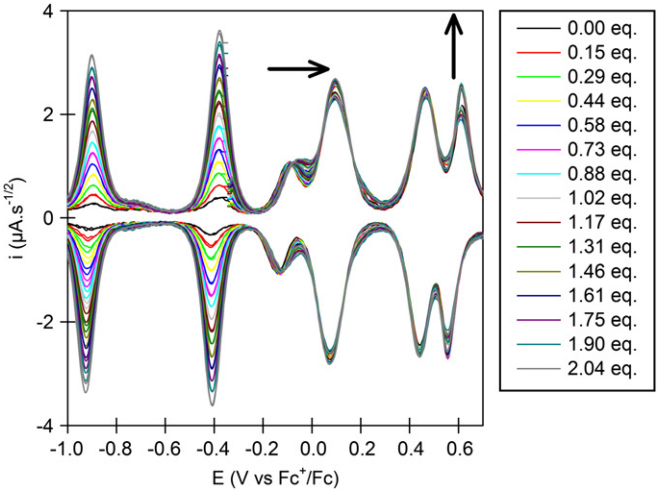

Figure 10. Deconvoluted cyclic voltammograms of receptor **1** (75 μM in CH_2Cl_2/toluene (8:2 v/v)) recorded at 200 mV s^{-1} after the addition of successive aliquots of MNTDMFC **4** (reference electrode: Fc^+/Fc; supporting electrolyte: TBAHFP (0.1 M)).

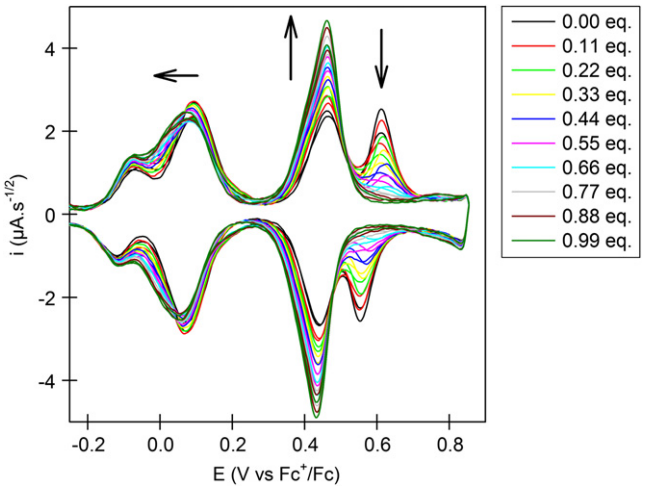

Figure 11. Deconvoluted cyclic voltammograms of complex (**4**$_2$⊂**1**) (75 μM in CH_2Cl_2/toluene (8:2 v/v)) at 200 mV s^{-1} obtained after the addition of successive aliquots of TBACl. Reference electrode: Fc^+/Fc; supporting electrolyte: *n*-Bu_4NPF_6 (0.1 M).

the successive addition of **4**. However, no significant effect on the potential of these reduction peaks was observed.

The addition of chloride to the complex **4**$_2$⊂**1** produces electrochemical effects similar to those observed for receptor **1** alone, i.e., a decrease in the separation (from ΔE=164 to 144 mV) and the complete disappearance of the peak ascribed to electrode absorption (Fig. 11). The negative shift of the first oxidation process indicates that the donor/acceptor interaction between compound **4** and the receptor is no longer present after the addition of chloride anion. Such a conclusion is in full agreement with the spectroscopic results discussed above and further supports the basic premise that the addition of chloride anion leads both to the break up of the complex **4**$_2$⊂**1** and to the formation of **1**·Cl^-.

2.5. Complexation between the receptor 1·Cl^- and the spherical guests 5 and 6

The interactions between receptor **1** and the spherical guests **5** and **6** were investigated in solution using absorption and emission spectroscopies, as well as cyclic voltammetry. The results of these studies are detailed below.

2.5.1. *Absorption spectroscopic investigations*

As noted above, the UV–vis absorption spectrum (recorded in dichloromethane) of receptor **1** in its 1,3-alternate conformation (Fig. 12B) did not reveal any appreciable bands at $\lambda \geq 550$ nm. Likewise, no significant absorption features were seen at $\lambda \geq 650$ nm in the absorption spectrum (Fig. 12B) of **5**. These solutions thus appear yellow (Fig. 12D) and magenta (Fig. 12E), respectively. In analogy to what was discussed previously, the addition of 5 equiv of TBACl to a dichloromethane solution of receptor **1** serves to shift the 1,3-alternate conformation to the cone conformation. Although this chloride-mediated conformational change is readily visualized by ^{1}H NMR spectroscopy, it does not give rise to any appreciable change in the color of the solution; thus, solutions of **1**·Cl^- also appear yellow. However, when 0.5 equiv of C_{60} **5** is added to the yellow solution of **1**·Cl^-, the color of the solution turns green (Fig. 12G) instantaneously. The absorption spectrum (Fig. 12B) of this solution displays a strong CT band having λ_{max}=725 nm (ε=1900 M^{-1} cm^{-1}). This diagnostic spectroscopic feature is most readily accounted for by the formation of a well-ordered, multicomponent supramolecular ensemble, **5**⊂(**1**·Cl^-)$_2$, wherein one molecule of C_{60} is encapsulated by two sets of the chloride-bound

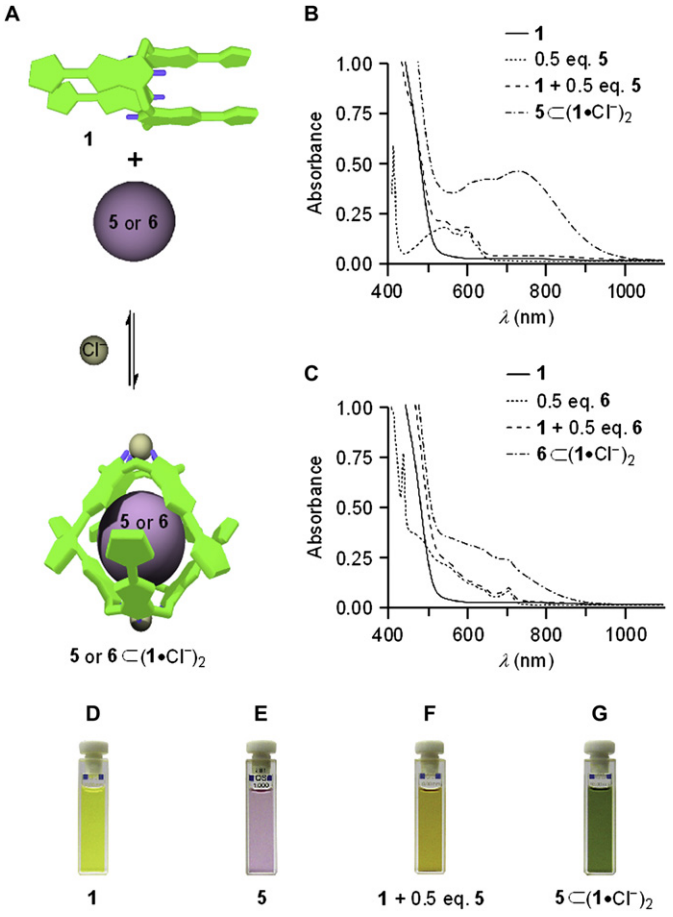

Figure 12. (A) Mechanistic scheme illustrating the proposed complex formation between receptor **1** and guest **5** or **6** in the presence of chloride anions. (B) Absorption spectra recorded in CH_2Cl_2 at 298 K of receptor **1** (0.4 mM), guest **5** (0.2 mM), receptor **1**+0.5 equiv of guest **5**, and of receptor **1**+0.5 equiv of guest **5**+2 equiv of TBACl. (C) Absorption spectra of receptor **1** (0.4 mM), guest **6** (0.2 mM), receptor **1**+0.5 equiv of guest **6**, and of receptor **1**+0.5 equiv of guest **6**+2 equiv of TBACl. Solutions in CH_2Cl_2 of (D) **1**, (E) **5**, (F) **1**+0.5 equiv of guest **5**, and (G) **1**+0.5 equiv of guest **5**+2 equiv of TBACl.

receptor (**1**·Cl^-, Fig. 12A). Presumably, the formation of this ensemble reflects an appropriate size and shape matching, as well as favorable CT interactions between the electron-rich TTF donor units and the electron-accepting C_{60} moiety.

As a control experiment, 0.5 equiv of C_{60} **5** was added to a dichloromethane solution of receptor **1** made up in the absence of chloride anion. This results in a color change from yellow to brown (Fig. 12F). This solution was characterized by the presence of a weak and broad absorption band centered at around λ_{max}=748 nm in the visible spectral region (Fig. 12B), a finding that is consistent with the presence of only a minimal intermolecular interaction between C_{60} and receptor **1** in its 1,3-alternate conformation.

Similar transformations are observed when 0.5 equiv of the spherical guest NMF (**6**) are added to the yellow solution of the receptor **1**·Cl^-; again, the color of the solution turns green. However, in this case, the CT band (Fig. 12C) appearing at λ_{max}=630 nm (ε=1408 M^{-1} cm^{-1}) is somewhat reduced compared to that of the **5**⊂(**1**·Cl^-)$_2$ ensemble. This reduction in absorption intensity is thought to reflect the fact that the supramolecular ensemble formed from **1**·Cl^- and **6**, namely **6**⊂(**1**·Cl^-)$_2$, is less-ordered than the ensemble **5**⊂(**1**·Cl^-)$_2$ as a result of both destabilizing steric interactions involving the TTF moieties of receptor **1** and the pyrrolidine substituted C_{60} moiety and a lower electronic coupling provided by substrate **6** as compared to **5**.

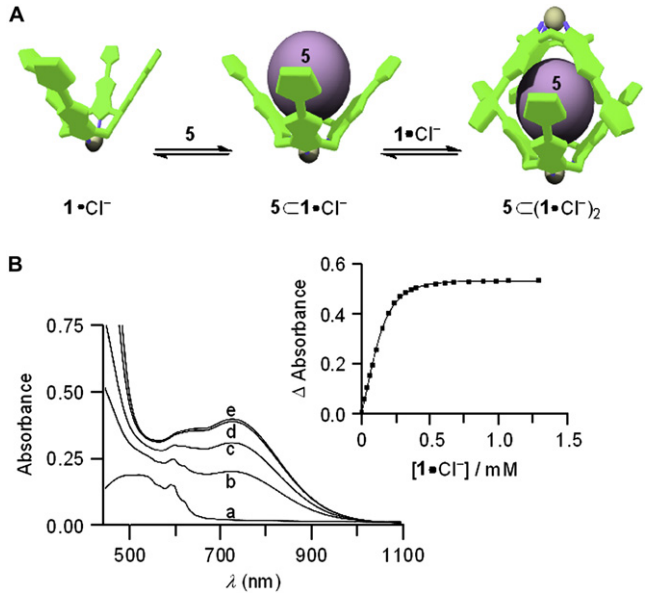

Figure 13. (A) Schematic representation of the equilibrium corresponding to the formation of $\mathbf{5}\subset\mathbf{1}\cdot Cl^-$ and $\mathbf{5}\subset(\mathbf{1}\cdot Cl^-)_2$. (B) Absorption spectra recorded in CH_2Cl_2 at 298 K of (a) **5** (0.2 mM), (b) $\mathbf{5}+\mathbf{1}\cdot Cl^-$ (0.5 equiv), (c) $\mathbf{5}+\mathbf{1}\cdot Cl^-$ (1.0 equiv), (d) $\mathbf{5}+\mathbf{1}\cdot Cl^-$ (2.0 equiv), and (e) $\mathbf{5}+\mathbf{1}\cdot Cl^-$ (6.0 equiv). The inset shows the changes in the CT band at 725 nm observed upon titration of **5** with $\mathbf{1}\cdot Cl^-$ in CH_2Cl_2 at 298 K.

A Job plot analysis of the interaction between $\mathbf{1}\cdot Cl^-$ and **5** in dichloromethane produced a curve with a maximum around a mole ratio of 0.35, a finding that is consistent with the formation of a 2:1 complex between $\mathbf{1}\cdot Cl^-$ and **5** as proposed above.

To determine the binding constants (K_1 and K_2) leading to the formation (Fig. 13A) of the putative 2:1 complex between $\mathbf{1}\cdot Cl^-$ and **5**, a UV–vis titration experiment, shown in Figure 13B, was carried out. In this experiment, the change in the intensity of the CT band (λ_{max}=725 nm) was monitored as increasing quantities of $\mathbf{1}\cdot Cl^-$ (preformed in dichloromethane, vide supra) were added to a dichloromethane solution of **5** at 298 K. After adding 2 equiv of $\mathbf{1}\cdot Cl^-$ to this solution, a saturation point was reached (Fig. 13B, d), with no perceptible changes being observed as additional equivalents of $\mathbf{1}\cdot Cl^-$ were added (Fig. 13B, e). The binding profile obtained from this experiment (Fig. 13B, inset) was subjected to standard nonlinear (2:1 host/guest) curve fitting analysis;[29] this gave binding constants of $K_1=2.3\times10^3\ M^{-1}$ and $K_2=1.3\times10^4\ M^{-1}$, reflecting the formation of $\mathbf{5}\subset\mathbf{1}\cdot Cl^-$ and $\mathbf{5}\subset(\mathbf{1}\cdot Cl^-)_2$, respectively. A similar UV–vis titration experiment, carried out using $\mathbf{1}\cdot Cl^-$ and guest **6**, gave rise to binding constants of $K_1=1.9\times10^3\ M^{-1}$ and $K_2=8.6\times10^2\ M^{-1}$ for the formation of $\mathbf{6}\subset\mathbf{1}\cdot Cl^-$ and $\mathbf{6}\subset(\mathbf{1}\cdot Cl^-)_2$, respectively.

2.5.2. Photophysical investigations

A gradual decrease in the steady state fluorescence spectral intensity ($\Phi=2.0\times10^{-4}$) of C_{60} (**5**) was also seen when increasing quantities of $\mathbf{1}\cdot Cl^-$ was added to dichloromethane solutions of the spherical electron-deficient species. This decrease is attributed to an electron transfer process evolving from the singlet excited state of **5**. As in the case of the absorption-based studies, the change in intensity could be used to determine the association constants for the formation of the successive $\mathbf{5}\subset\mathbf{1}\cdot Cl^-$ and $\mathbf{5}\subset(\mathbf{1}\cdot Cl^-)_2$ complexes. Specifically, changes in intensity (recorded at 690 nm) were plotted versus the $\mathbf{1}\cdot Cl^-$ concentration and fitted to standard binding profiles. The values obtained in this way, 2.4×10^3 and $2.8\times10^4\ M^{-1}$ for K_1 (i.e., $\mathbf{5}\subset\mathbf{1}\cdot Cl^-$) and K_2 (i.e., $\mathbf{5}\subset(\mathbf{1}\cdot Cl^-)_2$), respectively, are in a good agreement with those determined from the UV–vis titrations described above.

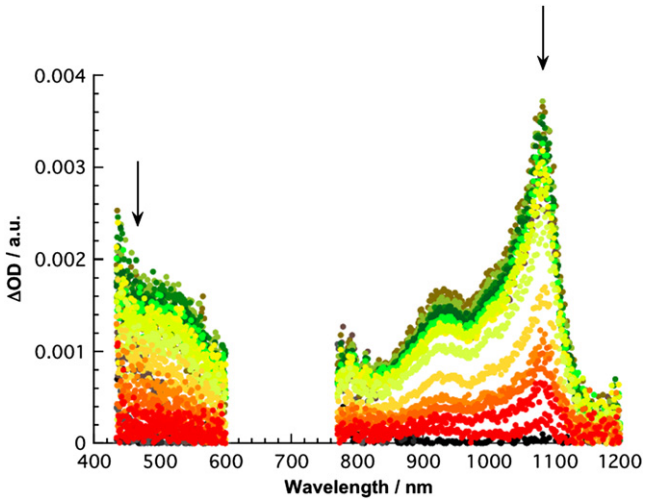

Figure 14. Differential absorption spectra (visible and near-infrared) obtained upon femtosecond flash photolysis (740 nm) of $\mathbf{5}\subset(\mathbf{1}\cdot Cl^-)_2$ in nitrogen saturated CH_2Cl_2 with several time delays between 0 and 10 ps at room temperature—arrows indicate the evolution of differential changes.

In addition, the fluorescence spectra recorded at the end of the titrations (i.e., at the plateau value of each assay) were evaluated to assess the dynamics of the excited state deactivation. In the tightly organized $\mathbf{5}\subset(\mathbf{1}\cdot Cl^-)_2$ complex, a quenching factor of 17 ($\Phi=1.1\times10^{-5}$) relative to free **5** leads to an appreciably fast electron transfer rate of $1.4\times10^{10}\ s^{-1}$ relative to the intrinsic decay of the singlet excited state decay of **5** (i.e., intersystem crossing rate of $8\times10^8\ s^{-1}$).

Transient absorption spectroscopy (cf. Fig. 14) provided support for this proposed electron transfer mechanism. In particular, femtosecond excitation into the CT absorption bands revealed features corresponding to the one-electron reduced fullerene radical anion at 1080 nm and the one-electron oxidized TTF radical cation, a species that is known to absorb at 400 nm. By mapping the radical ion pair formation rate to a first order kinetic model, we determined a rather fast electron transfer rate in the order of $10^{12}\ s^{-1}$, a value that is in good agreement with that obtained from an extrapolation of the steady state fluorescence quenching studies discussed above. Consistent with the proposed strong electron-donor/acceptor interactions in $\mathbf{5}\subset(\mathbf{1}\cdot Cl^-)_2$, the resulting radical ion pair is short-lived with a lifetime of only 3.1 ps.

For $\mathbf{6}\subset(\mathbf{1}\cdot Cl^-)_2$, femtosecond excitation into the CT absorption band at 730 nm revealed features that are superimposable with the sum of the one-electron reduced C_{60} (i.e., maximum at 1020 nm) and the one-electron oxidized TTF (i.e., in the 400 nm range). In general, analogous behavior was seen when 387 nm (a wavelength that effects C_{60} excitation) laser pulses were employed. However, under these latter conditions, an ultrashort transient, which bears close resemblance to the C_{60} singlet excited state at around 900 nm, was observed. This signal transforms rapidly to produce what is believed to be a radical ion pair. Consistent with the strong electron-donor interactions seen for $\mathbf{5}\subset(\mathbf{1}\cdot Cl^-)_2$, this putative radical ion pair is short-lived with a lifetime of only 5.6 ps.

2.5.3. Electrochemical investigations

Electrochemical measurements (Fig. 15) of **5**, $\mathbf{1}\cdot Cl^-$, and $\mathbf{5}\subset(\mathbf{1}\cdot Cl^-)_2$ in dichloromethane provided further support for the proposed binding events. In particular, the half-wave potential associated with the first reduction of the fullerene in $\mathbf{5}\subset(\mathbf{1}\cdot Cl^-)_2$ was found to be shifted to a more negative potential, as compared to that seen for the first reduction of free **5**. From an inspection of Figure 15B, it can be seen that the displacement of the first

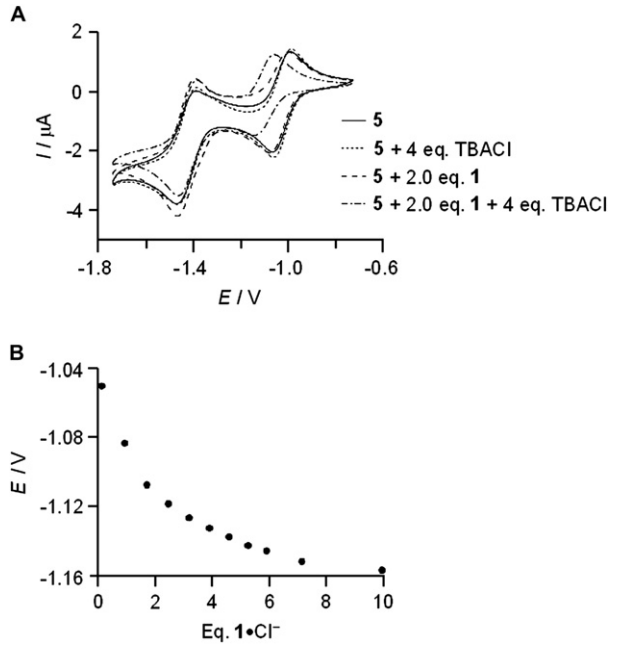

Figure 15. (A) Cyclic voltammograms recorded in CH_2Cl_2 at 298 K of **5** (0.2 mM), **5**+TBACl (4 equiv), **5**+**1** (2 equiv), and **5**+**1** (2 equiv)+TBACl (4 equiv). (B) CV titration curves (CH_2Cl_2, 0.2 mM) showing the negative shift of the first reduction potential of C_{60} **5** observed upon the addition of increasing amounts of **1**·Cl^-. In both cases, the reference electrode was Fc^+/Fc and the supporting electrolyte was TBAHFP (0.1 M).

reduction potential reaches a limit (ΔE=−106 mV) at the point where approximately 10 molar equiv of **1**·Cl^- have been added to a solution of the spherical guest **5**. Such a finding is fully consistent with a partial shift of electron density from the electron-donating TTF subunits to the bound guest **5**. The unusually high shift seen for the half-wave potential of **5** also serves to corroborate the strong electronic coupling that is proposed to exist within the self-assembled host/guest complex **5**⊂(**1**·Cl^-)$_2$.

When a mixture of dichloromethane and toluene (8:2 v/v) was used as the solvent, the addition of C_{60} to a solution of tetraTTF-calix[4]pyrrole **1** does not lead to any notable change in the receptor-based signals. However, as above, the successive addition of C_{60} to preformed solutions of **1**·Cl^- in this solvent mixture gives rise to clearly discernible variations in the potentials of the TTF

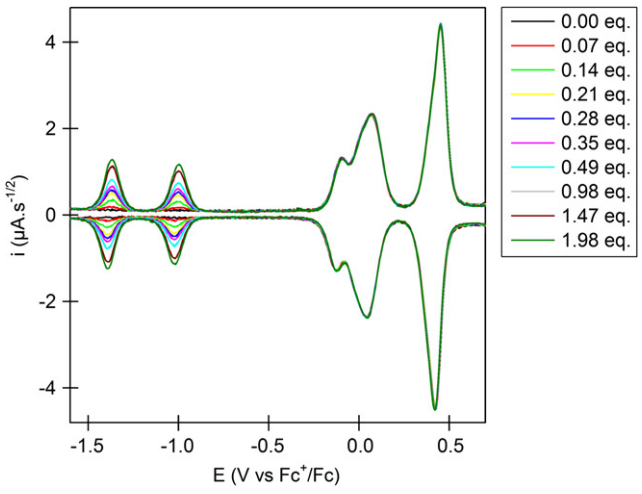

Figure 16. Deconvoluted cyclic voltammograms of complex **1**·Cl^- (75 μM in CH_2Cl_2/toluene (8:2 v/v)) at 200 mV s^{-1} obtained after the addition of successive aliquots of C_{60} (**5**). Reference electrode: Fc^+/Fc; supporting electrolyte: TBAHFP (0.1 M).

subunits in the receptor and the C_{60} guest (see Fig. 16). This experimental observation is not in agreement with the previous −106 mV shift in the first reduction process of the fullerene seen in pure dichloromethane. While this disparity is the subject of ongoing study, it is currently ascribed to what are fundamentally different experimental conditions, namely the presence or absence of toluene, a solvent that is believed to interact differently with C_{60} than dichloromethane.

2.6. Conformational control of receptor 1 leads to the selection between quasi-planar and spherical guests

Addition of 2 equiv of MTNDMFC **4** (Fig. 17E) and 0.5 equiv of **5** (Fig. 17F) to a dichloromethane solution of **1** (Fig. 17D) resulted in an immediate color change from yellow to brown (Fig. 17G). This was accompanied by the appearance of three CT bands centered at λ_{max}=525, 720, and 1220 nm (ε=3290, 1830, and 2624 M^{-1} cm^{-1}), respectively, in the absorption spectrum (Fig. 17B). These changes are ascribed to the recognition of two MTNDMFC **4** guests by receptor **1** in its anion-free 1,3-alternate conformation—a finding that is in agreement with previous experiments (cf. Fig. 7D). In analogy with what was observed earlier, the addition of 2 equiv of TBACl to this solution results in a conformational change to **1**·Cl^-. As true for other quasi-planar electron-deficient substrates considered in this study, this conformational change leads (Fig. 17A) to the break up of the complex **4**$_2$⊂**1**; however, in this case the presence of C_{60}, **5**, in the solution leads to the formation of a new 1:2 complex, namely **5**⊂(**1**·Cl^-)$_2$, that involves the spherical guest **5** and **1**·Cl^-. This transformation can be followed readily by the naked eye since the color of the solution changes from brown to green (Fig. 17H). There is also a large decrease in the absorption bands (Fig. 17B) centered at λ_{max}=525 and 1220 nm and the appearance of a new band centered at λ_{max}=735 nm (ε=1515 M^{-1} cm^{-1}, Fig. 17B), which originates from the 1:2 complex **5**⊂(**1**·Cl^-)$_2$, as seen above.

Extracting the TBACl salt from the dichloromethane phase by washing with water serves to regenerate the CT complex **4**$_2$⊂**1**. As a consequence, the brown color associated with this species is reestablished (Fig. 17I). However, the addition of a new aliquot of TBACl serves to convert receptor **1** into the chloride-bound cone conformation (i.e., complex **1**·Cl^-), which is then capable of binding C_{60} (**5**), again in a 1:2 fashion (i.e., to produce complex **5**⊂(**1**·Cl^-)$_2$). This results in a color change from brown to green (Fig. 17J).

Similar experiments involving this same quasi-planar electron-deficient guest (i.e., MTNDMFC, **4**) and the functionalized fullerene acceptor **6** were also carried out. Addition of 2 equiv of **4** and 0.5 equiv of the near-spherical guest **6** (Fig. 17C) to a dichloromethane solution of **1** produced an immediate color change from yellow to brown (Fig. 17N), as expected for the formation of **4**$_2$⊂**1**. The subsequent addition of 2 equiv of TBACl to this solution led, as above, to a color change from brown to green (Fig. 17O), a huge decrease in the intensity of the absorption bands centered at λ_{max}=525 and 1220 nm (Fig. 17C), and the appearance of a band centered at λ_{max}=630 nm (ε=2065 M^{-1} cm^{-1}). Such changes are consistent with the addition of TBACl to the original solution producing a conformational change in receptor **1** from its anion-free 1,3-alternate form to the corresponding anion-bound cone conformation, complex **1**·Cl^-, which results, as above, in decomplexation of **4** from complex **4**$_2$⊂**1** and formation of the 1:2 complex **6**⊂(**1**·Cl^-)$_2$.

2.7. Complexation between the bifunctional guest 7 and the receptor 1

The complexation between the receptor **1** and the dyad TNDCF–C_{60} **7** was investigated under two different scenarios each of which

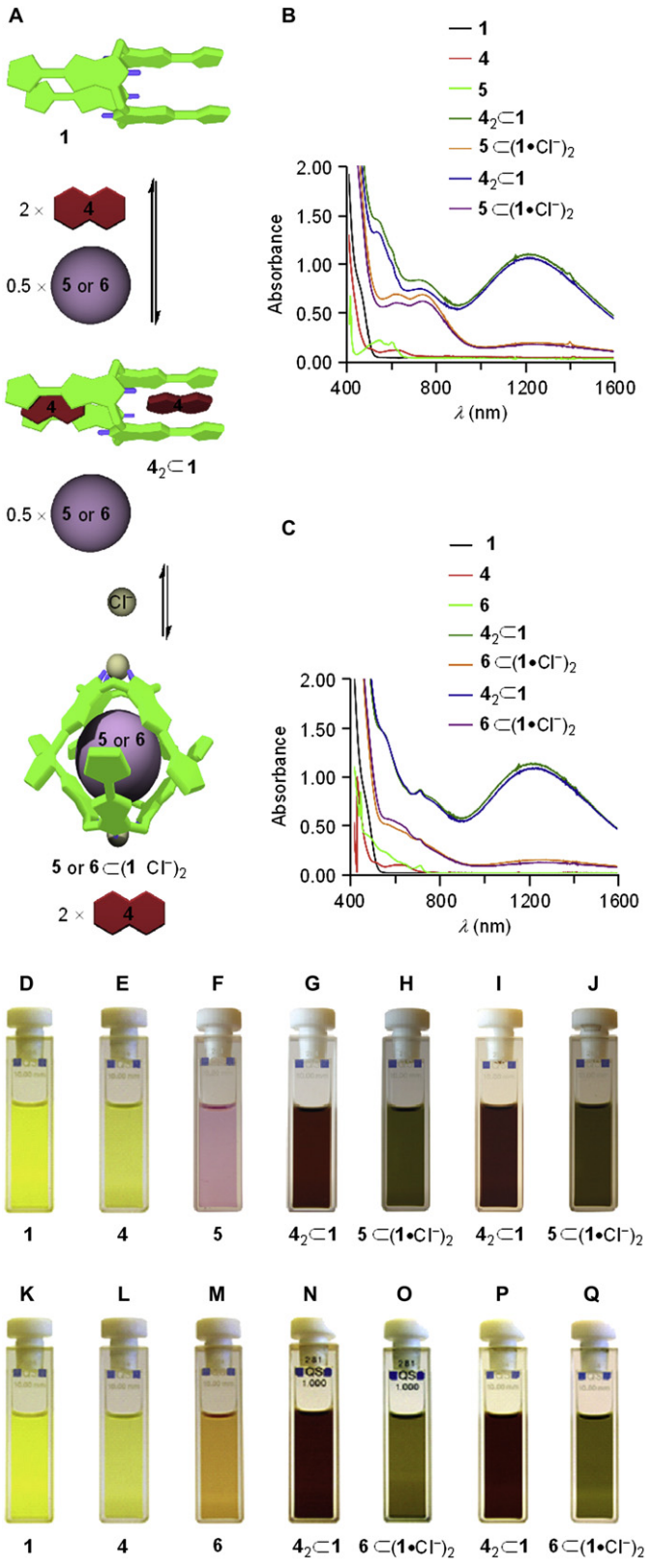

Figure 17. (A) Mechanistic scheme illustrating the proposed complexation events involving receptor **1** and guests **4** and **5**, as well as guests **4** and **6**, as observed in the absence and presence of chloride anions, respectively. (B) and (C) Absorption spectra recorded in CH_2Cl_2 at 298 K. (D)–(J) Pictures of CH_2Cl_2 solutions of **1** (0.4 mM), **4** (0.8 mM), **5** (0.2 mM), complex $\mathbf{4}_2\subset\mathbf{1}$, complex $\mathbf{5}\subset(\mathbf{1}\cdot Cl^-)_2$, and complex $\mathbf{5}\subset(\mathbf{1}\cdot Cl^-)_2$ after being subject to a water wash, and complex $\mathbf{5}\subset(\mathbf{1}\cdot Cl^-)_2$ after the addition of a second aliquot of chloride anion. (K)–(Q) Pictures of CH_2Cl_2 solutions of receptor **1** (0.4 mM), **4** (0.8 mM), **6** (0.2 mM), complex $\mathbf{4}_2\subset\mathbf{1}$, complex $\mathbf{6}\subset(\mathbf{1}\cdot Cl^-)_2$, and complex $\mathbf{6}\subset(\mathbf{1}\cdot Cl^-)_2$ after being subject to a water wash, and complex $\mathbf{6}\subset(\mathbf{1}\cdot Cl^-)_2$ after the addition of a second aliquot of TBACl.

was designed to optimize the interactions between the bifunctional guest and the receptor in its two limiting conformations, **1** and $\mathbf{1}\cdot Cl^-$. In the first scenario (Figs. 18 and 19), the stoichiometry between the receptor **1** and the guest **7** was adjusted to a 1:2 molar ratio. Under these conditions (Fig. 18A), a complex, $\mathbf{7}_2\subset\mathbf{1}$, is formed wherein receptor **1**, in its anion-free 1,3-alternate conformation, accommodates 2 molar equiv of guest **7** as a result of binding to the quasi-planar TNDCF 'tails'. In the second scenario (Fig. 20), which involves pre-addition of chloride anion, the ratio between receptor **1** (essentially fully converted to $\mathbf{1}\cdot Cl^-$) and **7** was adjusted to a 2:1 stoichiometry. This results in the formation of a complex, $\mathbf{7}\subset(\mathbf{1}\cdot Cl^-)_2$, wherein receptor **1** in its cone conformation $\mathbf{1}\cdot Cl^-$ encapsulates the spherical fullerene 'head' of a single guest **7**. Support for these assignments, which are correlated with very different optical 'read-outs', came from a variety of spectroscopic analyses as detailed below. For ease of understanding, the results

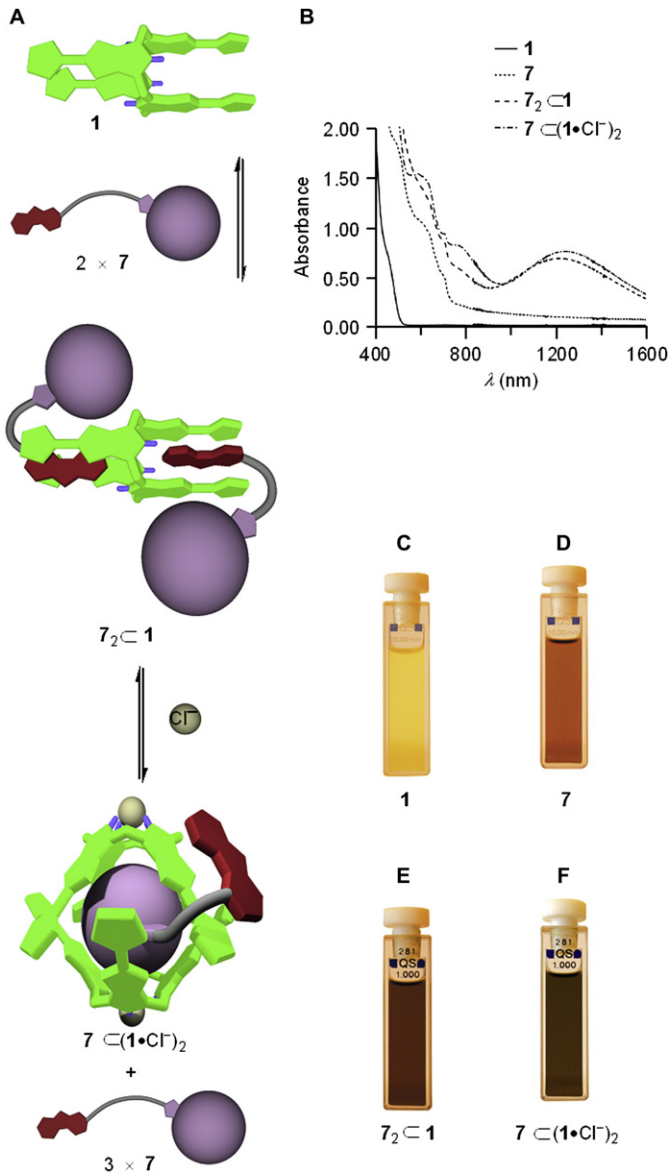

Figure 18. (A) Mechanistic scheme illustrating the proposed binding of the bidentate guest **7** to, and partial release from, receptor **1** observed in the absence and presence of chloride anions, respectively, under conditions where the guest/receptor ratio is 2:1. (B) Absorption spectra recorded in CH_2Cl_2 at 298 K. (C)–(F) Pictures of CH_2Cl_2 solutions of **1** (0.133 mM), **7** (0.266 mM), complex $\mathbf{7}_2\subset\mathbf{1}$, and complex $\mathbf{7}\subset(\mathbf{1}\cdot Cl^-)_2$.

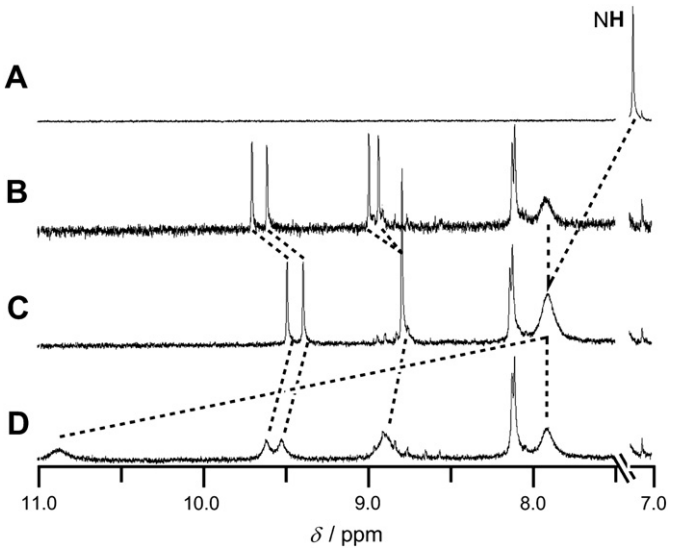

Figure 19. Partial ^{1}H NMR spectra (500 MHz) recorded in $CDCl_3$ at 298 K of (A) receptor **1** (0.3 mM), (B) guest **7** (0.6 mM), (C) receptor **1**+2 equiv of guest **7**, and (D) receptor **1**+2 equiv of guest **7**+2 equiv of TBACl.

from these studies are presented in the context of two limiting scenarios.

2.7.1. Scenario 1

First, the complexation between receptor **1** and the dyad TNDCF–C_{60} **7** was investigated in solution using UV–vis and near IR absorption and ^{1}H NMR spectroscopies. As noted previously, the absorption spectrum (Fig. 18B) of receptor **1** (in its anion-free 1,3-alternate conformation) did not reveal any visible absorption bands at λ>550 nm and the solution appears yellow (Fig. 18C). The dyad TNDCF–C_{60} **7** showed absorptions in the λ=400–800 nm spectral region with only a very weak absorptions being observed for 800<λ<1600 nm; dilute dichloromethane solutions of this compound thus appear light brown (Fig. 18D). On the other hand, the addition of 2 equiv[30] of guest **7** to such solutions of **1** results in an immediate color change from yellow to dark brown (Fig. 18E), as would be expected for the formation of a 2:1 CT complex $\mathbf{7}_2\subset\mathbf{1}$. The absorption spectrum (Fig. 18B, $\mathbf{7}_2\subset\mathbf{1}$) of this solution showed a strong CT band centered at λ_{max}=1216 nm (ε=2500 $M^{-1}\,cm^{-1}$). Such an observation is rationalized in terms of the proposed stabilizing donor/acceptor interactions between the electron-rich TTF units present in receptor **1** and the electron-deficient TNDCF moiety of guest **7** and is in agreement with the previous findings and conclusions (cf. Fig. 7D and accompanying discussion).

Addition of 2 equiv of chloride anions to a solution of the complex $\mathbf{7}_2\subset\mathbf{1}$ results in a chloride-mediated conformational change of the receptor (Fig. 18A) to the anion-bound cone conformation ($\mathbf{1}\cdot Cl^-$). As in the case of the analogous experiments discussed above, this change in conformation occurs essentially instantaneously and is observed as a color change from dark brown to a more greenish color (Fig. 18F). Analysis of the absorption spectrum (Fig. 18B, $\mathbf{7}\subset(\mathbf{1}\cdot Cl^-)_2$) reveals an increase in the absorption for the CT band centered at λ_{max}=757 nm, corresponding to the complexation of $\mathbf{1}\cdot Cl^-$ and the C_{60} moiety of the guest **7**. A small increase in intensity and a bathochromic shift in the band corresponding to the CT interaction (λ_{max}=1239 nm, ε=2800 $M^{-1}\,cm^{-1}$, Fig. 18B) between the receptor **1** and the TNDCF moiety of the bidentate receptor **7** are also observed. This finding is rationalized in terms of the TNDCF-part of **7**, even though it is no longer complexed by receptor **1**, being held in close proximity to the TTF units through the glycol linker. This results in an ancillary interaction giving rise to the pronounced CT band centered at λ_{max}=1239 nm.

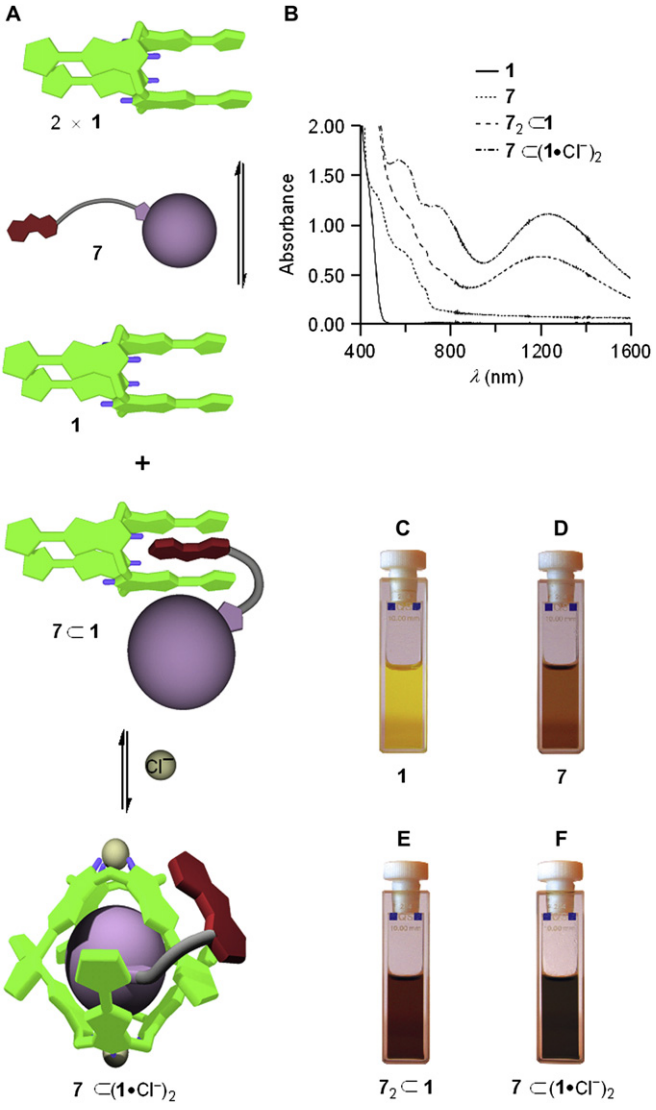

Figure 20. (A) Mechanistic scheme illustrating the proposed binding of the bidentate guest **7** to, and partial release from, receptor **1** observed in the absence and presence of chloride anions, respectively, under conditions where the guest/receptor ratio is 1:2. (B) Absorption spectra recorded in CH_2Cl_2 at 298 K. (C)–(F) Pictures of CH_2Cl_2 solutions of **1** (0.4 mM), **7** (0.2 mM), the complex $\mathbf{7}\subset\mathbf{1}$, and the complex $\mathbf{7}\subset(\mathbf{1}\cdot Cl^-)_2$.

Putting these secondary effects aside, the key point is that the differential response to substrate **7** elicited by Cl^- may be followed easily by monitoring the naked eye-detectable changes in the color of the solution.

Further support for the proposed switching events came from ^{1}H NMR spectroscopic analyses. As noted previously, the ^{1}H NMR spectrum of receptor **1** (shown again in Fig. 19A) reveals a signal at δ=7.15 ppm, which corresponds to the NH proton resonances. For the bifunctional substrate, dyad **7**, four Ar–H signals, arising from the TNDCF moiety, appear as four doublets at δ=9.71, 9.62, 9.00, and 8.94 ppm (J=1.4 Hz), while the Ar–H resonances from the benzene ring are seen as two signals at δ=8.13 and 8.11 ppm and as a broad peak at δ=7.93 ppm (Fig. 19B). Upon addition of 2 equiv of guest **7** to a solution of receptor **1** (Fig. 19C) in its anion-free 1,3-alternate conformation, the signals corresponding to the NH protons are seen to shift to δ=7.91 ppm ($\Delta\delta$=0.78 ppm), as would be expected given the proposed hydrogen bonding interactions between the host and the guest(s). In this mixture, the Ar–H protons of guest **7** are shifted upfield ($\Delta\delta$=−0.14–0.22 ppm), presumably, as a consequence of being sandwiched between two shielding TTF subunits.

Upon addition of 2 molar equiv of chloride anion, the signals for the Ar–H protons in **7** become broadened. They also shift to lower field. However, they do not recover fully to their initial positions, a finding consistent with the proposed outside binding of the TNDCF portion of the substrate, as inferred from the optical studies discussed immediately above. This subtlety notwithstanding, it is important to appreciate that the addition of chloride anion serves to release the quasi-planar TNDCF 'tail' of guest **7** from within the sandwich-like complex $\mathbf{7}_2\subset\mathbf{1}$ as a consequence of the conformational switching of the tetraTTF-calix[4]pyrrole receptor **1** from its anion-free 1,3-alternate form to the corresponding anion-bound cone conformation ($\mathbf{1}\cdot Cl^-$). Additionally, the NH protons in receptor **1** are seen to shift to lower field (δ=10.82 ppm, Fig. 19D) upon the addition of Cl^- in accord with what was seen above.

2.7.2. Scenario 2

To probe further the properties of the present multi-component, multi-functional system, the binding effects were explored under a second scenario, namely one where a 2:1 ratio between the receptor **1** and the guest **7** was used (Fig. 20). In this case, the absorption spectrum revealed a strong CT band centered at λ_{max}=1212 nm (ε=850 $M^{-1}\,cm^{-1}$). Addition of 2 equiv of chloride anion to this solution again serves to shift the 1,3-alternate conformation of the receptor **1** to its cone conformation $\mathbf{1}\cdot Cl^-$, a process that can be followed by a color change from brown to green. Under these conditions, a large increase in the absorption band centered at λ_{max}=747 nm (ε=1500 $M^{-1}\,cm^{-1}$, Fig. 20B), corresponding to the complexation of the C_{60} 'head' of substrate **7** within the bowl-like cavity of receptor $\mathbf{1}\cdot Cl^-$, is observed. An increase in the absorption intensity and a bathochromic shift (λ_{max}=1240 nm, ε=1400 $M^{-1}\,cm^{-1}$, Fig. 20B) in the CT band, ascribed to the interactions between receptor **1** and the TNDCF moiety of guest **7**, are also seen. Thus, as in Section 2.7.1, the various chemical inputs associated with this set of experimental conditions are readily detectable in terms of easy-to-see changes in optical 'outputs'.

2.7.3. Determination of binding constants using absorption spectroscopy

To determine the binding constants (K_1 and K_2) for the 2:1 complexation[31] of $\mathbf{1}\cdot Cl^-$ with the C_{60}-part of the guest TNDCF–C_{60} **7** (i.e., C_{60}-part of $\mathbf{7}\subset(\mathbf{1}\cdot Cl^-)_2$), a UV–vis spectroscopic titration (Fig. 21) was carried out. This involved monitoring the changes in the absorbance of the CT bands centered at λ_{max}=747 and 1090 nm upon the addition of increasing amounts of $\mathbf{1}\cdot Cl^-$ to a dichloromethane solution of **7** at 298 K. After the addition of 2 equiv of $\mathbf{1}\cdot Cl^-$ to solution **7**, a saturation point was reached (Fig. 21) and only small changes were observed in the absorption spectra after this point. The change in absorbance for the CT band (λ_{max}=1090 nm) was plotted (Fig. 21, inset) as a function of added $\mathbf{1}\cdot Cl^-$. The experimental data were subjected to a standard nonlinear curve fitting analysis (Connors 1:2 binding model),[29,32] allowing values of 2.8×10^3 and 1.3×10^4 M^{-1} to be determined for K_1 (i.e., C_{60}-part of $\mathbf{7}\subset\mathbf{1}\cdot Cl^-$) and K_2 (i.e., C_{60}-part of $\mathbf{7}\subset(\mathbf{1}\cdot Cl^-)_2$), respectively. Interestingly, in this case, $K_2>K_1$, even though **7** is a fulleropyrrolidine derivative; presumably, this reflects the additional 'out-side' interactions between receptor $\mathbf{1}\cdot Cl^-$ and this bifunctional substrate.

2.7.4. Photophysical investigations

To complement the binding assays the fluorescence features of the TNDCF and C_{60} subunits in **7** were followed as a function of its interaction with **1** in its 1,3-alternate and cone conformations. Implicit in these analyses, since they involve excited states, are electron transfer reactions that are expected to be dependent on the nature of the electron-accepting guest (i.e., TNDCF) and the electron-donating receptor **1**.

When variable concentrations of **1** are added to **7** a trend evolves that is essentially identical to what is seen for **4**–**6** (vide supra). In particular, following the changes in the TNDCF fluorescence at 710 nm allowed binding constants of 2.8×10^3 and 7.1×10^3 M^{-1} to be calculated for complexes $\mathbf{7}\subset\mathbf{1}$ and $\mathbf{7}_2\subset\mathbf{1}$, respectively.

The interactions between **7** and $\mathbf{1}\cdot Cl^-$ were also tested using emission spectroscopic methods. In this case, the observed changes in fluorescence intensity were used to determine the association constants for the successive formation of $\mathbf{7}\subset(\mathbf{1}\cdot Cl^-)$ and $\mathbf{7}\subset(\mathbf{1}\cdot Cl^-)_2$. Toward this end, the change in fluorescence intensity at 710 nm was plotted versus the concentration of $\mathbf{1}\cdot Cl^-$. This gave rise to calculated values, 8.3×10^3 and 1.2×10^4 M^{-1} for K_1 (i.e., $\mathbf{7}\subset(\mathbf{1}\cdot Cl^-)$) and K_2 (i.e., $\mathbf{7}\subset(\mathbf{1}\cdot Cl^-)_2$), respectively, which were in agreement with those determined from the absorption assays noted above and those determined by fluorescence for pure C_{60} (cf., Section 2.5.2).

Gratifyingly, complexes $\mathbf{7}_2\subset\mathbf{1}$ and $\mathbf{7}\subset(\mathbf{1}\cdot Cl^-)_2$ have different optical signatures. As a result, their selective excitation could be effectively 'tuned' in transient absorption measurements. In analogy to the photoreactivity of $\mathbf{4}_2\subset\mathbf{1}$, transient absorption features observed following the 775 or 1200 nm excitation of $\mathbf{7}_2\subset\mathbf{1}$ included the radical anion bands of the one-electron reduced TNDCF at 535 and 870 nm (cf. Fig. 22). Subjecting the decay traces to a first

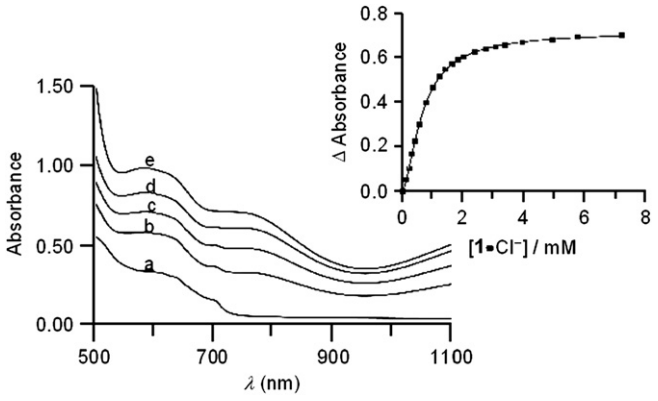

Figure 21. (A) Absorption spectra recorded in CH_2Cl_2 at 298 K of (a) **7** (0.2 mM), (b) $\mathbf{7}+\mathbf{1}\cdot Cl^-$ (0.6 equiv), (c) $\mathbf{7}+\mathbf{1}\cdot Cl^-$ (1.0 equiv), (d) $\mathbf{7}+\mathbf{1}\cdot Cl^-$ (2.1 equiv), and (e) $\mathbf{7}+\mathbf{1}\cdot Cl^-$ (7.5 equiv). Inset shows the changes in the CT band at 1090 nm observed upon titration of **7** with $\mathbf{1}\cdot Cl^-$.

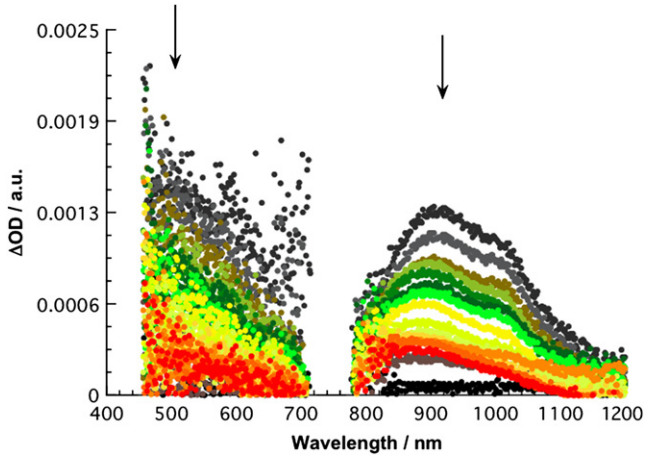

Figure 22. Differential absorption spectra (visible and near-infrared) obtained upon femtosecond flash photolysis (775 nm) of $(\mathbf{7})_2\subset\mathbf{1}$ in nitrogen saturated CH_2Cl_2 with several time delays between 0 and 10 ps at room temperature; arrows indicate the evolution of the differential response.

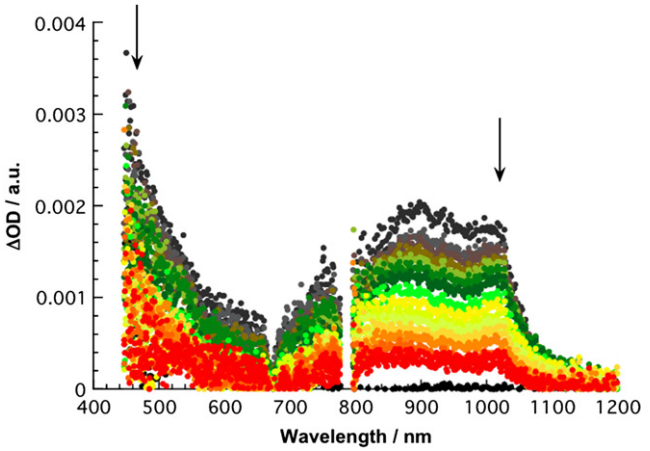

Figure 23. Differential absorption spectra (visible and near-infrared) obtained upon femtosecond flash photolysis (730 nm) of $\mathbf{7}\subset(\mathbf{1}\cdot Cl^-)_2$ in nitrogen saturated CH_2Cl_2 with several time delays between 0 and 10 ps at room temperature; arrows indicate the evolution of the differential response.

order kinetic equation, afforded a 2.4 ps lifetime for the underlying radical ion pair state.

Finally, we confirmed that an electron transfer mechanism governs the excited state deactivation in $\mathbf{7}\subset(\mathbf{1}\cdot Cl^-)_2$. This was done by subjecting the complex to femtosecond excitation at 730 nm, which corresponds to the CT absorption band. The resulting transients revealed features that clearly match those for the one-electron reduced radical anion of C_{60} and the one-electron oxidized radical cation of TTF (i.e., features at 1020 and 400 nm, respectively) (see Fig. 23). Using a first order kinetic equation, a lifetime of 3.7 ps was determined for the metastable radical ion pair state. On the other hand, excitation at 1200 nm did not reveal any absorption features, something that one would expect there was an appreciable interaction between the TTF subunits and the bound TNDCF guests.

2.7.5. *Electrochemical investigations*

The electrochemical behavior of compound **1** during the successive addition of the dyad **7**, studied in a mixture of dichloromethane and toluene (8:2 v/v), was quite similar to that seen upon the addition of compound **4**, i.e., a positive shift in the peak ascribed to the first oxidation process and the appearance of an absorption peak during the second oxidation process. These results are consistent with the quasi-planar aromatic portion of the dyad being complexed by receptor **1**; they are thus fully in agreement with those inferred from the spectroscopic studies detailed above.

As was previously observed in the case of $\mathbf{4}_2\subset\mathbf{1}$, the addition of chloride to complex $\mathbf{7}_2\subset\mathbf{1}$ induces a decrease in the separation of the first oxidation process and a near-elimination of the peak ascribed to absorption effects; again, these findings are best interpreted in terms of **1** undergoing a conformation change from the 1,3-alternate to the corresponding cone conformation. However, it is noteworthy that no appreciable shift in the reduction potential of the C_{60} moiety is observed during the successive addition of Cl^- to $\mathbf{7}_2\subset\mathbf{1}$. This may reflect relatively weak interactions or other effects that have yet to be detailed.

3. Conclusion

In conclusion, we have shown that the tetraTTF-calix[4]pyrrole **1** acts as a sandwich-like receptor molecule for electron-deficient guests in its 1,3-alternate conformation **1** and as a cage-like receptor molecule for spherical electron-deficient guests in its anion-bound cone conformation $\mathbf{1}\cdot Cl^-$. The addition of chloride ions serves to affect the release of quasi-planar, electron-deficient guests from the 1,3-alternate conformation. However, this same addition and conformational switching abets the binding of more spherical electron-deficient guests in the resulting anion-bound cone conformation. The dynamic nature of receptor **1** makes it a versatile scaffold for studying donor and acceptor interactions between TTF and electron-deficient guests within a well-defined unimolecular system. These same structural features also make receptor **1** near-unique in that it acts as a very simple anion-triggered molecular switch. Currently, efforts are underway to generalize the findings presented herein via the synthesis of new, modified calix[4]pyrrole TTF derivatives.

Acknowledgements

We gratefully acknowledge the Lundbeckfonden for a Postdoctoral scholarship to K.A.N., as well as financial support provided by the Danish Natural Science Research Council through the SONS Programme of the European Science Foundation, which is also funded by the European Commission, Sixth Framework Programme and the Danish Natural Science Research Council (SNF, projects #21-03-0317 and #21-02-0414) in Denmark. The work in Spain was supported by the Spanish Government CICYT (grant MAT2005-07369-C03-2 and Consolider Ingenio 2010 project HOPE CSD2007-00007). The work in Austin was supported by the National Science Foundation (grant CHE-0515670 to JLS) and the Robert A. Welch Foundation (grant F-1018 to JLS). The work in Angers was supported by the Centre National de la Recherche Scientifique (CNRS—France), the 'Agence Nationale de la Recherche' (ANR—France), and the 'Région des Pays de la Loire' (France). The work in Erlangen was supported by the Deutsche Forschungsgemeinschaft (SFB 583) and the Office of Basic Energy Sciences of the U.S. Department of Energy.

Supplementary data

Details of spectroscopic analyses and determinations of K_a values. Supplementary data associated with this article can be found in the online version, at doi:10.1016/j.tet.2008.05.141.

References and notes

1. Baeyer, A. *Ber. Dtsch. Chem. Ges.* **1886**, *19*, 2184–2185.
2. Gale, P. A.; Sessler, J. L.; Král, V.; Lynch, V. *J. Am. Chem. Soc.* **1996**, *118*, 5140–5141.
3. (a) Gale, P. A.; Genge, J. W.; Král, V.; McKervey, M. A.; Sessler, J. L.; Walker, A. *Tetrahedron Lett.* **1997**, *38*, 8443–8444; (b) Bonomo, L.; Solari, E.; Toraman, G.; Scopelliti, R.; Floriani, C.; Latronico, M. *Chem. Commun.* **1999**, 2413–2414; (c) Anzenbacher, P., Jr.; Jursíková, K.; Lynch, V. M.; Gale, P. A.; Sessler, J. L. *J. Am. Chem. Soc.* **1999**, *121*, 11020–11021; (d) Camiolo, S.; Gale, P. A. *Chem. Commun.* **2000**, 1129–1130; (e) Bucher, C.; Zimmerman, R. S.; Lynch, V.; Sessler, J. L. *J. Am. Chem. Soc.* **2001**, *123*, 9716–9717; (f) Woods, C. J.; Camiolo, S.; Light, M. E.; Coles, S. J.; Hursthouse, M. B.; King, M. A.; Gale, P. A.; Essex, J. W. *J. Am. Chem. Soc.* **2002**, *124*, 8644–8652; (g) Dukh, M.; Drasar, P.; Cerny, I.; Pouzar, V.; Shriver, J. A.; Král, V.; Sessler, J. L. *Supramol. Chem.* **2002**, *14*, 237–244; (h) Yoon, D.-W.; Hwang, H.; Lee, C.-H. *Angew. Chem., Int. Ed.* **2002**, *41*, 1757–1759; (i) Sessler, J. L.; Cho, W.-S.; Lynch, V.; Král, V. *Chem.—Eur. J.* **2002**, *8*, 1134–1143; (j) Lee, C.-H.; Na, H.-K.; Yoon, D.-W.; Won, D.-H.; Cho, W.-S.; Lynch, V. M.; Shevchuk, S. V.; Sessler, J. L. *J. Am. Chem. Soc.* **2003**, *125*, 7301–7306; (k) Bucher, C.; Zimmerman, R. S.; Lynch, V.; Sessler, J. L. *Chem. Commun.* **2003**, 1646–1647.
4. Bucher, C.; Zimmerman, R. S.; Lynch, V.; Král, V.; Sessler, J. L. *J. Am. Chem. Soc.* **2001**, *123*, 2099–2100.
5. (a) Miyaji, H.; Anzenbacher, P., Jr.; Sessler, J. L.; Bleasdale, E. R.; Gale, P. A. *Chem. Commun.* **1999**, 1723–1724; (b) Anzenbacher, P., Jr.; Jursíková, K.; Sessler, J. L. *J. Am. Chem. Soc.* **2000**, *122*, 9350–9351; (c) Miyaji, H.; Sato, W.; Sessler, J. L. *Angew. Chem., Int. Ed.* **2000**, *39*, 1777–1780; (d) Miyaji, H.; Sato, W.; Sessler, J. L.; Lynch, V. M. *Tetrahedron Lett.* **2000**, *41*, 1369–1373; (e) Miyaji, H.; Sato, W.; An, D.; Sessler, J. L. *Collect. Czech. Chem. Commun.* **2004**, *69*, 1027–1049.
6. (a) Sessler, J. L.; Gebauer, A.; Gale, P. A. *Gazz. Chim. Ital.* **1997**, *127*, 723–726; (b) Gale, P. A.; Hursthouse, M. B.; Light, M. E.; Sessler, J. L.; Warriner, C. N.; Zimmerman, R. S. *Tetrahedron Lett.* **2001**, *42*, 6759–6762.
7. Nielsen, K. A.; Jeppesen, J. O.; Levillain, E.; Becher, J. *Angew. Chem., Int. Ed.* **2003**, *42*, 187–191.

8. (a) Bryce, M. R. *J. Mater. Chem.* **2000**, *10*, 589–598; (b) Segura, J. L.; Martín, N. *Angew. Chem., Int. Ed.* **2001**, *40*, 1372–1409; (c) Jeppesen, J. O.; Becher, J. *Eur. J. Org. Chem.* **2003**, 3245–3266; (d) Becher, J.; Jeppesen, J. O.; Nielsen, K. A. *Synth. Met.* **2003**, *133 and 134*, 309–315; (e) Jeppesen, J. O.; Nielsen, M. B.; Becher, J. *Chem. Rev.* **2004**, *104*, 5115–5131.
9. For other examples of chemosensors based on TTF, see: (a) Heuzé, K.; Mézière, C.; Fourmigué, M.; Batail, P.; Coulon, C.; Canadell, E.; Auban-Senzier, P.; Jérome, D. *Chem. Mater.* **2000**, *12*, 1898–1904; (b) Trippe, G.; Levillain, E.; Derf, F. L.; Gorgues, A.; Sallé, M.; Jeppesen, J. O.; Nielsen, K.; Becher, J. *Org. Lett.* **2002**, *4*, 2461–2464; (c) Lyskawa, J.; Derf, F. L.; Levillain, E.; Mazari, M.; Salle, M.; Dubois, L.; Viel, P.; Bureau, C.; Palacin, S. *J. Am. Chem. Soc.* **2004**, *126*, 12194–12195; (d) Trippe, G.; Derf, F. L.; Lyskawa, J.; Mazari, M.; Roncali, J.; Gorgues, A.; Levillain, E.; Salle, M. *Chem.—Eur. J.* **2004**, *10*, 6497–6509; (e) Zhao, B.-T.; Blesa, M.-J.; Mercier, N.; Derf, F. L.; Salle, M. *New J. Chem.* **2005**, *29*, 1164–1167; (f) Lu, H.; Xu, W.; Zhang, D.; Chen, C.; Zhu, D. *Org. Lett.* **2005**, *7*, 4629–4632; (g) Lu, H.; Xu, W.; Zhang, D.; Zhu, D. *Chem. Commun.* **2005**, 4777–4779.
10. (a) Bucher, C.; Seidel, D.; Lynch, V.; Král, V.; Sessler, J. L. *Org. Lett.* **2000**, *2*, 3103–3106; (b) Král, V.; Sessler, J. L.; Zimmerman, R. S.; Seidel, D.; Lynch, V.; Andrioletti, B. *Angew. Chem., Int. Ed* **2000**, *39*, 1055–1058.
11. Nielsen, K. A.; Cho, W.-S.; Jeppesen, J. O.; Lynch, V. M.; Becher, J.; Sessler, J. L. *J. Am. Chem. Soc.* **2004**, *126*, 16296–16297.
12. (a) Nielsen, K. A.; Cho, W.-S.; Sarova, G. H.; Petersen, B. M.; Bond, A. D.; Becher, J.; Jensen, F.; Guldi, D. M.; Sessler, J. L.; Jeppesen, J. O. *Angew. Chem., Int. Ed.* **2006**, *45*, 6848–6853; (b) Nielsen, K. A.; Sarova, G. H.; Martín-Gomis, L.; Fernández-Lázaro, F.; Stein, P. C.; Sanguinet, L.; Levillain, E.; Sessler, J. L.; Guldi, D. M.; Sastre-Santos, Á.; Jeppesen, J. O. *J. Am. Chem. Soc.* **2008**, *130*, 460–462.
13. Nielsen, K. A.; Cho, W.-S.; Lyskawa, J.; Levillain, E.; Lynch, V. M.; Sessler, J. L.; Jeppesen, J. O. *J. Am. Chem. Soc.* **2006**, *128*, 2444–2451.
14. Martín-Gomis, L.; Ortiz, J.; Fernández-Lázaro, F.; Sastre-Santos, Á.; Elliott, B.; Echegoyen, L. *Tetrahedron* **2006**, *62*, 2102–2109.
15. Cox, C. T., Jr.; Cooper, M. M. *J. Chem. Educ.* **2006**, *83*, 99–100.
16. $CDCl_3$ was used in the ^1H NMR spectroscopic studies.
17. Solvent conditions for the CV experiments were toluene/dichloromethane (8:2 v/v), a choice dictated by solubility considerations.
18. (a) Custelcean, R.; Moyer, B. A.; Sessler, J. L.; Cho, W.-S.; Gross, D.; Bates, G. W.; Brooks, S. J.; Light, M. E.; Gale, P. A. *Angew. Chem., Int. Ed.* **2005**, *44*, 2537–2542; *Angew. Chem.* **2005**, *117*, 2513–2518; (b) Sessler, J. L.; Gross, D. E.; Cho, W.-S.; Lynch, V. M.; Schmidtchen, F. P.; Bates, G. W.; Light, M. E.; Gale, P. A. *J. Am. Chem. Soc.* **2006**, *128*, 12281–12288; (c) Bates, G. W.; Gale, P. A.; Light, M. E. *CrystEngComm* **2006**, *8*, 300–302; (d) Bates, G. W.; Gale, P. A.; Light, M. E. *Supramol. Chem.* **2008**, *20*, 23–28; (e) Wintergerst, M. P.; Levitskaia, T. G.; Moyer, B. A.; Sessler, J. L.; Delmau, L. H. *J. Am. Chem. Soc.* **2008**, *130*, 4129–4139.
19. Jia, C.; Liu, S.-X.; Tanner, C.; Leiggener, C.; Sanguinet, L.; Levillain, E.; Leutwyler, S.; Hauser, A.; Decurtins, S. *Chem. Commun.* **2006**, 1878–1880.
20. Khodorkovsky, V.; Becker, J. Y. In *Organic Conductors: Fundamentals and Applications*; Farges, J.-P., Ed.; Marcel Dekker: New York, NY, 1994.
21. Bard, A. J.; Faulkner, L. R. *Electrochemical Methods. Fundamentals and Applications*; Wiley: New York, NY, 1980.
22. The advantage of ITC for monitoring the recognition of anionic guests by calix[4]pyrroles has been noted in the literature. See, for instance: Schmidtchen, F. P. *Org. Lett.* **2002**, *4*, 431–434.
23. A binding constant of $2.5\times10^6\ M^{-1}$ has previously been reported for the complexation of **1** with chloride ions in 1,2-dichloroethane (DCE) at 298 K, see Refs. 11 and 13.
24. In these experiments, it is expected that the binding interactions between the potassium cation—complexed by the dicyclohexane-18-crown-6—and the anion-bound receptor, $\mathbf{1}\cdot Cl^-$, are small compared to those between the TBA^+ cation and the receptor $\mathbf{1}\cdot Cl^-$.
25. Hexafluorophosphate was chosen as the counter anion, because all available evidence supports the notion that this anion has a very low affinity for receptor **1**.
26. In principle, hydrogen bonding interactions can also take place between the NH protons of the receptor **1** and the carbonyl and ester groups present in guests **3** and **4**.
27. See Supplementary data.
28. In the case of guest **4**, the experiment was carried out in the reverse order, giving a maximum at 0.30, such a finding is also interpreted in terms of a 1:2 binding stoichiometry between receptor **1** and guest **4**.
29. Connors, A. K. *Binding Constants: The Measurement of Molecular Complex Stability*; Wiley: New York, NY, 1987.
30. A continuous variation UV–vis experiment was carried out to determine the stoichiometry of the binding interaction between receptor **1** and the bifunctional substrate **7**. The resulting Job plot exhibited a maximum at a mole fraction of approximately 0.28. This is interpreted in terms of a 1:2 binding stoichiometry (1:7), see Supplementary data.
31. A continuous variation UV–vis experiment was carried out to determine the stoichiometry of the binding interaction between the preformed receptor chloride complex $\mathbf{1}\cdot Cl^-$ and the bifunctional substrate **7** in dichloromethane solution. The resulting Job plot exhibited a maximum at a molar fraction of approximately 0.37. This is interpreted in terms of a 2:1 binding ratio between $\mathbf{1}\cdot Cl-$ and **7**; see Supplementary data.
32. Estimated errors $<15\%$.